Rapid single crystal growth via guest displacement from host-guest complexes

Mikayla L. Horvath,[a] Caylee E. Jumbelic,[a] Rosemarie A. Burynski,[a] M. Brody Mistrot,[a]

Robert D. Pike,*[b] Brian J. Smith*[a] and Hasan Arslan*,[a]

[a] *Department of Chemistry, Bucknell University, Lewisburg, PA 17837, USA*
[b] *Department of Chemistry, William & Mary, Williamsburg, VA 23185, USA*

Supplementary Information

Correspondence Address

Professor Hasan Arslan
Department of Chemistry
Bucknell University
Lewisburg, PA 17837 (USA)
Tel: (+1)-570-577-1042
Fax: (+1)-570-577-1739
Email: hasan.arslan@bucknell.edu

Table of Contents

A. Materials. All reagents were purchased from commercial sources and used without further purification unless noted otherwise. Acetonitrile (MeCN) was distilled over CaH_2 and stored over 3Å molecular sieves. MeCN-d3 was purchased from Cambridge Isotope Laboratories and dried over 3Å molecular sieves. Other solvents were purchased from commercial sources and used without further purification. **ExBox·4TFSI**[1] was synthesized according to the literature procedures with minor modifications as outlined below.

Instrumentation.

Infrared spectra were recorded on a Thermo Nicolet iS10 with a diamond ATR attachment (Pike Technologies GladiATR). Ultraviolet/visible absorbance spectra were recorded on a Cary 60 spectrophotometer with a Xe lamp.

High resolution mass spectrometry was performed on an Agilent 6560 Ion Mobility Quadrupole/Time-of-Flight (IM-Q-ToF) Mass Spectrometer with Agilent Jet Stream dual electrospray ion source using positive ionization. Solutions of analytes were prepared in LC-MS grade MeCN with 0.1% formic acid (Fisher Optima). Mass-to-charge ratio calibration was performed on the same day, prior to sample data acquisition, using Agilent ESI-L tune mix diluted according to manufacturer guidelines.

NMR spectra were recorded on a Varian 400 MHz spectrometer with quad probe (^{1}H, ^{19}F, ^{31}P, ^{13}C), or a Varian 600 MHz spectrometer with broadband probe at 25 ℃ without spinning the sample. NMR titration data was used to build binding isotherms using BindFit v0.5 at http://supramolecular.org[2]

Optical microscopy imaging was done using a Nikon SMZ 1500 microscope and View 4K camera and InFocus software.

All X-ray measurements were made using graphite-monochromated Mo Kα radiation or microfocus Cu Kα radiation on a Bruker DUO three-circle diffractometer, equipped with an Apex II CCD detector. All data were collected at 100 K. Initial space group determination was based on a matrix consisting of 36 (Mo) or 90 (Cu) frames. The data were corrected for Lorentz and polarization[3] effects and absorption using SADABS.[4] All structures were solved using intrinsic phasing. Structure solution, refinement and the calculation of derived results were performed using the SHELXTL[5] package of software and ShelXl.[6] Non-hydrogen atoms were refined anisotropically. All hydrogen atoms were placed in theoretical positions. For **A-*t*Bu⊂ExBox·4PF$_6$** many of the anions and solvent molecules were found to be highly disordered and required extensive modelling. For **A-*t*Bu** data were collected for a two-component twin crystal, and twin integration and scaling software (as part of the SHELXTL package) was used to solve the structure from diffraction domains having about 70:30 populations.

B. Synthetic Procedures

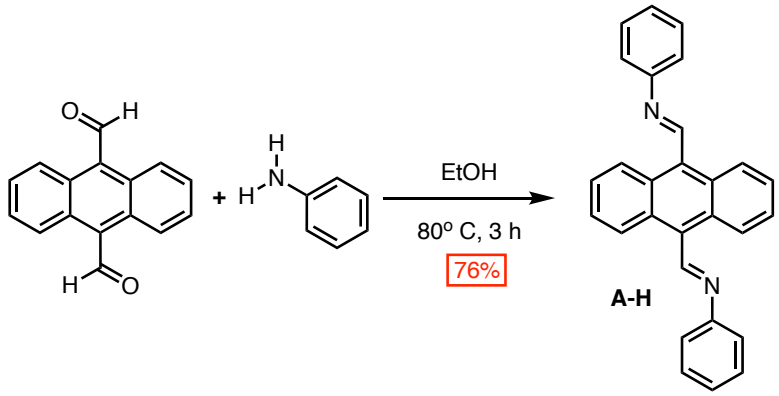

A-H: 9,10-Anthracenedicarboxaldehyde (0.0516 g, 0.226 mmol) was added to a 10 mL round-bottom flask with a stir bar. EtOH (2.5 mL) was added to dissolve the solid starting material, giving an orange solution. Aniline (0.062 g, 0.060 mL, 0.67 mmol) was added to the reaction flask, and the reaction was heated at reflux for 3 hours under a N_2 atmosphere. After the reaction was complete, the reaction mixture was cooled to room temperature, the precipitate was collected using vacuum filtration, and washed with cold EtOH (2×5 mL) to give **A-H** as a bright yellow solid (0.0656 g, 0.1706 mmol, 76% yield). **A-H:** ^{1}H NMR (400 MHz, $CDCl_3$) δ 9.67 (s, 2H), 8.72–8.65 (m, 4H), 7.64–7.57 (m, 4H), 7.53 (t, J = 7.5 Hz, 4H), 7.47 (d, J = 7.5 Hz, 4H), 7.37 (t, J = 7.5 Hz, 2H). ^{13}C NMR (100 MHz, $CDCl_3$) δ 160.12, 152.39, 131.15, 130.09, 129.56, 127.08, 126.82, 125.55, 121.23. IR (solid, ATR): 3085, 3047, 3030, 2965, 2869, 1625, 1611, 1586, 1575, 1523, 1481, 1448, 1263, 1206, 1177, 1168, 1157, 1149, 1074, 1048, 1020, 971, 952, 911, 900, 830, 800, 761, 754, 738, 697, 693, 669, 667, 620, 612, 605, 556, 528 cm^{-1}. HRMS (IM-Q-ToF, *m/z*): calcd for $[C_{28}H_{20}N_2+H]^+$ 385.1700, found 385.1730.

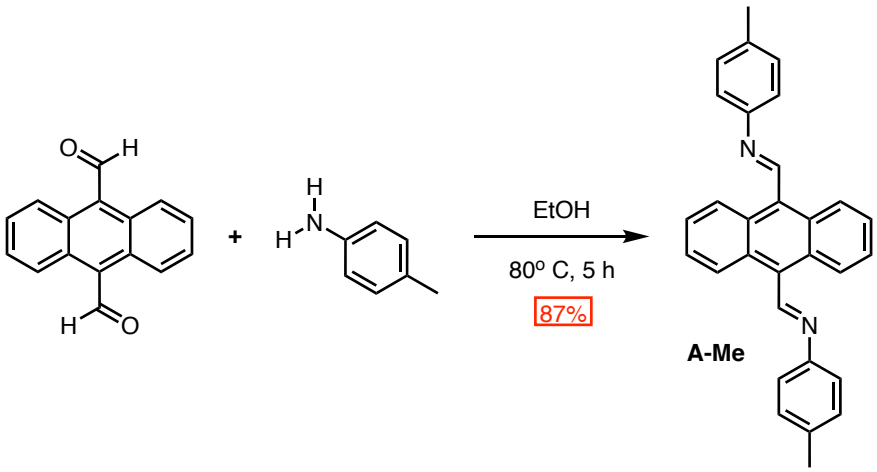

A-Me: 9,10-Anthracenedicarboxaldehyde (0.1002 g, 0.4277 mmol) and *p*-toluidine (0.1421 g, 1.326 mmol) were added to a 25 mL round-bottom flask with a stir bar. EtOH (4.3 mL) was added to dissolve the solid reactants, giving a bright orange mixture. The reaction was heated at reflux under a N_2 atmosphere. After 30 min, the reaction mixture was a turbid yellow suspension. After 5 hours, the mixture was removed from heat and allowed to cool to room temperature. The precipitate was collected using vacuum filtration, and washed with cold EtOH (2×5 mL) to give **A-Me** as a bright yellow powder (0.1532 g, 0.3714 mmol, 87% yield). **A-Me:** ^{1}H NMR (400 MHz, $CDCl_3$) δ 9.64 (s, 2H), 8.69–8.63 (m, 4H), 7.61–7.55 (m, 4H), 7.40 (d, J = 7.9 Hz, 4H), 7.33 (d, J

= 7.9 Hz, 4H), 2.46 (s, 6H). ^{13}C NMR (100 MHz, $CDCl_3$) δ 159.20, 149.83, 136.73, 131.15, 130.10, 130.04, 126.91, 125.55, 121.15, 21.23. IR (solid, ATR): 3026, 2919, 2870, 1622, 1614, 1597, 1502, 1442, 1338, 1212, 1205, 1176, 1167, 1048, 1016, 969, 901, 843, 829, 794, 765, 761, 751, 735, 710, 657, 642, 611, 606, 525, 508 cm^{-1}. HRMS (IM-Q-ToF, *m/z*): calcd for $[C_{30}H_{24}N_2+H]^+$ 413.2013, found 413.2052.

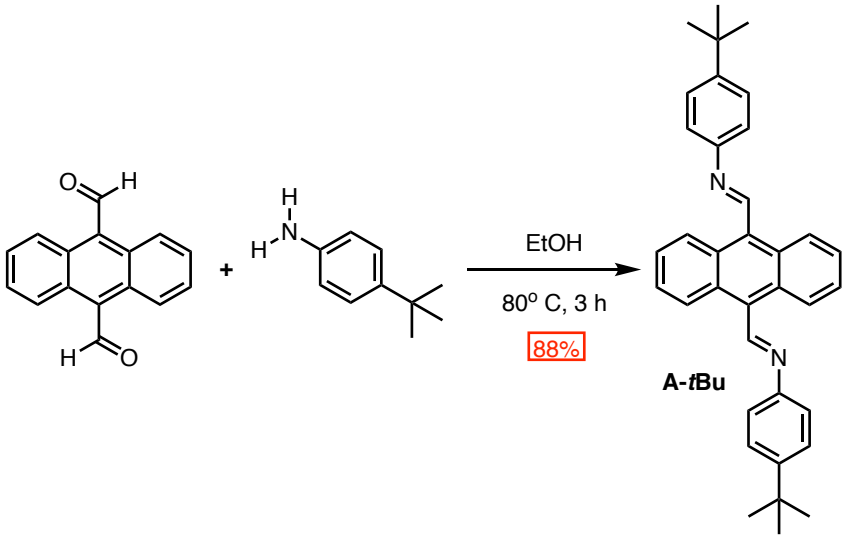

A-*t*Bu: 9,10-Anthracenedicarboxaldehyde (0.0516 g, 0.226 mmol) was added to a 10 mL round-bottom flask with a stir bar. EtOH (2.5 mL) was added to dissolve the solid starting material, giving an orange solution. 4-*t*-butylaniline (0.102g, 0.110 mL, 0.69 mmol) was added to the reaction flask, and the reaction was heated at reflux for 3 hours under a N_2 atmosphere. After the reaction was complete, the reaction mixture was cooled to room temperature, the precipitate was collected using vacuum filtration, and washed with cold EtOH (2×5 mL) to give **A-*t*Bu** as a bright orange solid (0.0959 g, 0.1931 mmol, 88% yield). **A-*t*Bu:** ^{1}H NMR (400 MHz, $CDCl_3$) δ 9.69 (s, 2H), 8.71 – 8.62 (m, 4H), 7.61–7.52 (m, 4H), 7.55 (d, J = 8.4 Hz, 4H), 7.44 (d, J = 8.4 Hz, 4H), 1.41 (s, 18H). ^{13}C NMR (100 MHz, $CDCl_3$) δ 159.29, 150.07, 149.64, 131.20, 130.05, 126.90, 126.41, 125.56, 120.95, 34.79, 31.61. IR (solid, ATR): 2950, 2904, 2873, 2361, 2332, 1613, 1589, 1495, 1443, 1366, 1360, 1268, 1173, 1116, 1051, 1011, 970, 903, 851, 839, 816, 796, 756, 736, 643, 558 cm^{-1}. HRMS (IM-Q-ToF, *m/z*): calcd for $[C_{36}H_{36}N_2+H]^+$ 497.2952, found 497.3007.

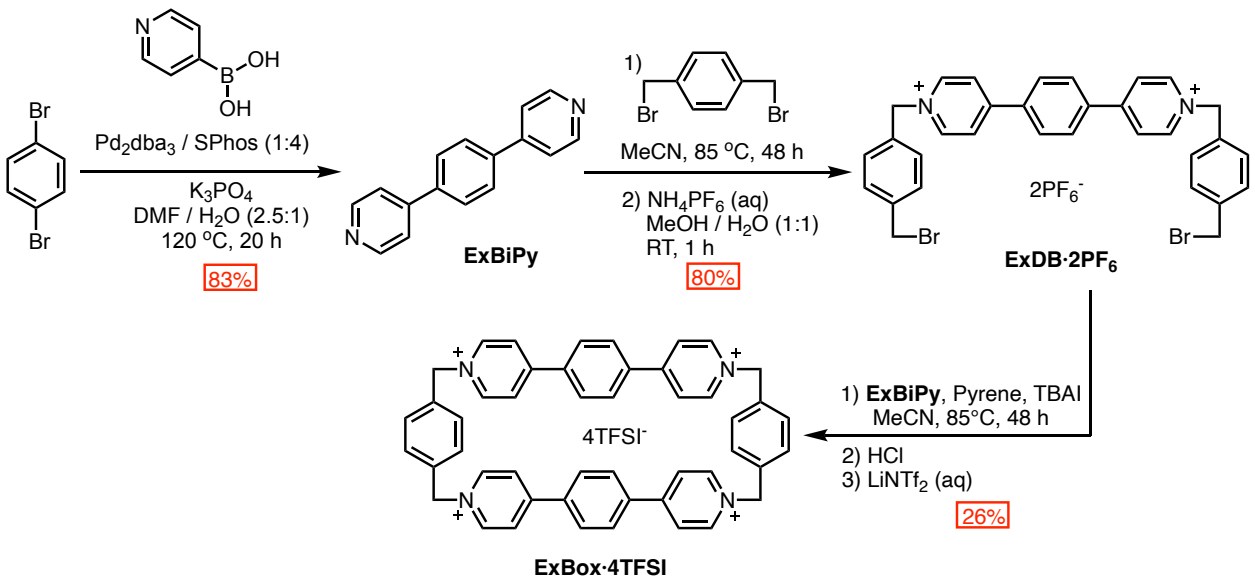

Scheme S1. Synthesis of **ExBox·4TFSI** from commercially available starting materials.

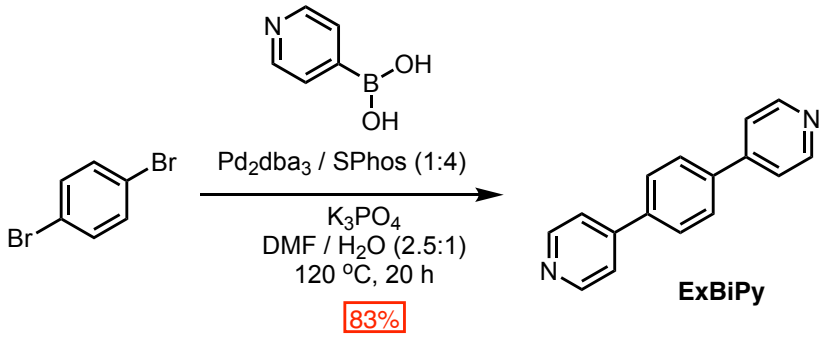

ExBiPy: 1,4-dibromobenzene (0.100 g, 0.424 mmol), 4-pyridine boronic acid (0.156 g, 0.127 mmol), potassium phosphate (0.270 g, 1.272 mmol), Pd_2dba_3 (0.004 g, 0.004 mmol), and Sphos (0.007 g, 0.017 mmol) were added to a 15 mL pressure flask with a stir bar. A mixture of DMF/H_2O (2.5:1 mL) was bubbled for 30 min and then added to the reaction flask using cannula transfer to form a grey-white suspension. The reaction was heated to 120 °C. After 15 min, all solid was dissolved, forming a brown solution. After 20 hours, the flask was removed from heat and allowed to cool to room temperature. The crude reaction mixture was transferred to an Erlenmeyer flask and the volume was raised to 50 mL with H_2O to form a white precipitate. The precipitate was collected by vacuum filtration and air-dried overnight to give **ExBiPy** as a white solid (0.0828 g, 0.356 mmol, 83% yield). **ExBiPy:** ^{1}H NMR (400 MHz, $CDCl_3$) δ 8.74 – 8.67 (m, 4H), 7.77 (s, 4H), 7.60 – 7.51 (m, 4H). This ^{1}H NMR spectrum is consistent with the one reported in the literature.[7]

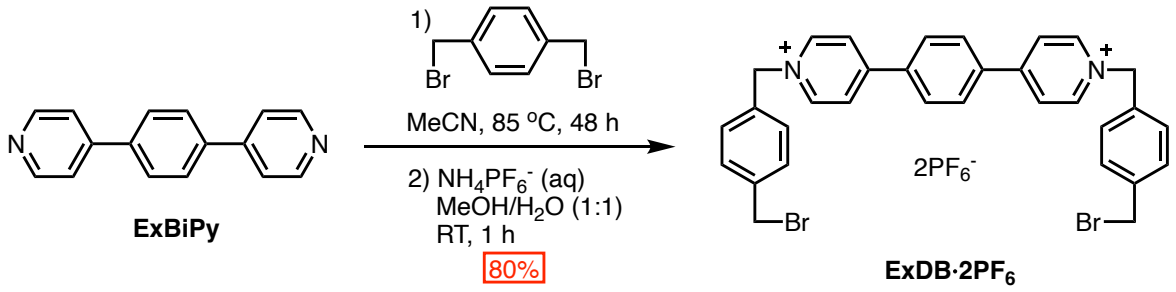

ExDB·2PF$_6$: *p*-Xylylene dibromide (5.6464 g, 21.39 mmol) and dry MeCN (100 mL) were added to a 250 mL round-bottom flask with a stir bar. The reaction was heated to reflux (85 °C) under a N_2 atmosphere, at which point *p*-xylylene dibromide dissolved. A suspension of **ExBiPy** (0.5058 g, 2.177 mmol) in MeCN (30 mL) was slowly added to the reaction flask in 6 mL increments 30 min apart. After 48 h, the reaction mixture was cooled down to room temperature, the pale-yellow precipitate was collected using vacuum filtration, and washed with $CHCl_3$ (3×50 mL) to give **ExDB·2Br**. The crude product was dissolved in 1:1 (*v*/*v*) MeOH/H_2O (100 mL). 0.2 M NH_4PF_6(aq) (38 mL, 7.6 mmol) was added, forming a white precipitate, and stirred at room temperature for 1 hour. The resulting precipitate was collected using vacuum filtration and dried under vacuum, giving **ExDB·2PF$_6$** as a white powder (1.5306 g, 1.719 mmol, 80% yield) **ExDB·2PF$_6$:** ^{1}H NMR (400 MHz, CD_3CN) δ 8.83 (d, J = 6.4 Hz, 4H), 8.34 (d, J = 6.4 Hz, 4H), 8.12 (s, 4H), 7.55 (d, J = 8.0 Hz, 4H), 7.47 (d, J = 8.0 Hz, 4H), 5.75 (s, 4H), 4.61 (s, 4H). This ^{1}H NMR spectrum is consistent with the one reported in the literature.[7]

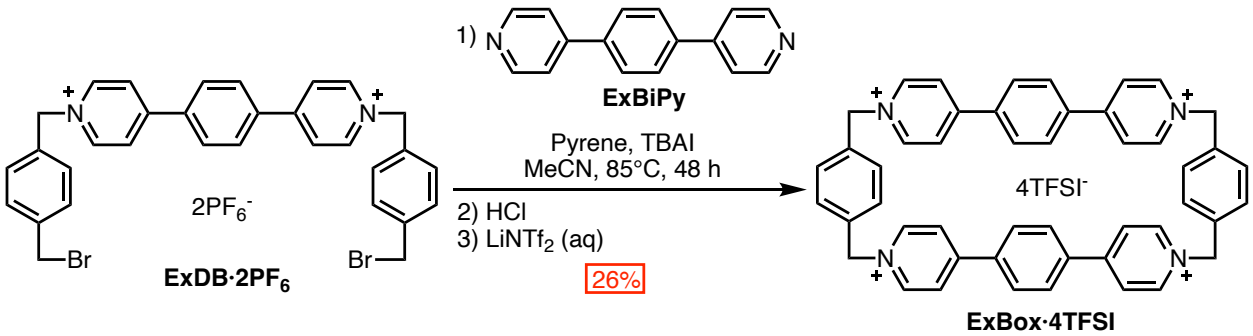

ExBox·4TFSI: Pyrene-templated synthesis of $ExBox^{4+}$ was carried out as follows: **ExDB·2PF$_6$** (0.8019 g, 0.9007 mmol), **ExBiPy** (0.2097 g, 0.9028 mmol), pyrene (1.0968 g, 5.4230 mmol), and TBAI (0.0671 g, 0.1817 mmol) were added to a 500 mL round-bottom flask with a stir bar, and dissolved in dry MeCN (180 mL). The reaction was heated at reflux under a N_2 atmosphere. After 48 hours, the reaction mixture turned into a yellow-orange suspension; concentrated HCl(aq) was added (1 mL, excess), resulting in further precipitate formation, and the mixture was cooled to room temperature. The crude product was collected using vacuum filtration and washed with chloroform (3×40 mL) to remove excess (unbound) pyrene. It was dissolved in DMSO (100 mL), diluted in H_2O (400 mL) and pyrene bound to $ExBox^{4+}$ was removed using continuous liquid-liquid extraction with $CHCl_3$ as the bottom layer. As pyrene was removed, the color of the aqueous layer changed from orange to clear. This layer was then collected and transferred to a 1 L Erlenmeyer flask. 1.0 M NH_4PF_6(aq) (10 mL, 10 mmol) was added to the Erlenmeyer flask and a precipitate crashed out of the solution immediately. The off-white precipitate was collected using vacuum filtration and washed with H_2O (3×50 mL)) and dried in air. An anion exchange from PF_6^- to Cl^- was performed by dissolving the crude product in MeCN (100 mL) and slowly adding this

solution to a stirring mixture of concentrated HCl (1.2 mL) in MeCN (20 mL). The off-white precipitate was collected using vacuum filtration and washed with MeCN (3×10 mL). It was mixed with celite in a mortar and pestle for dry-loading, and purified using flash column chromatography (SiO_2-C18Aq, 15% *v*/*v* MeCN/H_2O). . Combined $ExBox^{4+}$ fractions were precipitated using 1.0 M LiTFSI(aq) (5 mL, 5.0 mmol), and collected using vacuum filtration to give **ExBox·4TFSI** as a white powder (0.4259 g, 0.2375 mmol, 26% yield). **ExBox·4TFSI:** ^{1}H NMR (400 MHz, CD_3CN) δ 8.78 (d, *J* = 7.1 Hz, 8H), 8.17 (d, *J* = 7.1 Hz, 8H), 7.93 (s, 8H), 7.60 (s, 8H), 5.69 (s, 8H). This ^{1}H NMR spectrum is consistent with the one reported in the literature.[7]

C. Single Crystal Growths

The following protocol was used for the set-up of each single crystal growth attempt involving guest displacement. A saturated solution of the guest compound was prepared in a 1.0 mL solution of **ExBox·4TFSI** (5.00 mM, MeCN) by sonication. This process typically resulted in a noticeable color change due to charge transfer bands between the host and the guest, a reliable indicator for the formation of host-guest complexes. The excess solid was removed by filtering this mixture through a 0.22 μm hydrophilic PTFE filter, and the solution was transferred to a 1 mL glass culture tube (ID = 5mm). 0.1 mL of a pyrene solution (57 mM, MeCN) was injected with a long needle into the bottom of the culture tube to form a layer underneath the host-guest complex solution. The small culture tube was placed inside a 20 mL scintillation vial, which was capped and sealed with parafilm to allow for undisturbed crystal growth on benchtop at room temperature. Single crystal formation typically started within minutes, and was complete in 2-3 hours.

A group of anthracene and anthraquinone derivatives were used to investigate the scope of the guest displacement crystal growth: **A-H**, **A-Me**, **A-*t*Bu**, 9,10-bis(phenylethynyl)anthracene (**BPA**), anthrarufin, anthraquinone, 1,5-dichloroanthraquinone (**DCAQ**), alizarin, and anthracene-9,10-dicarbaldehyde (**ADC**) (Chart S1). Formation of the host-guest complexes between these guests and $ExBox^{4+}$ were observed using ^{1}H-NMR spectroscopy as shown in section F below.

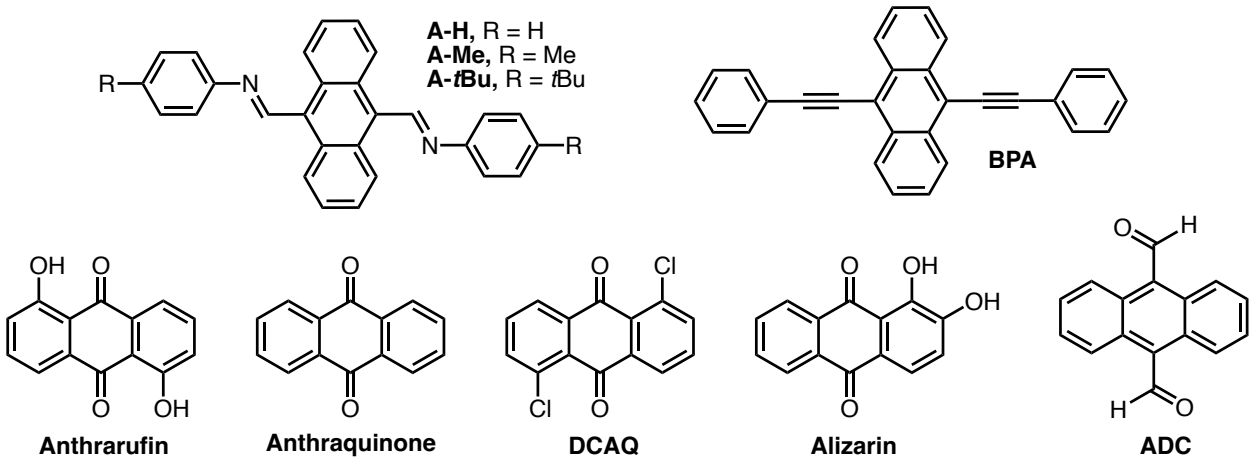

Chart S1. Guest compounds studied in crystal growth experiments.

Table S1: Single crystal structure data of **A-Me** and **A-*t*Bu**.

	A-Me	**A-*t*Bu**
Formula	$C_{30}H_{24}N_2$	$C_{36}H_{36}N_2$
Formula weight	412.51	496.67
Space group	$P2_1/c$	$P\bar{1}$
Crystal system	Monoclinic	Triclinic
a (Å)	16.2355(7)	6.1032(13)
b (Å)	5.7098(3)	8.943(2)
c (Å)	11.9788(5)	13.218(3)
α (deg)	90	79.840(4)
β (deg)	102.9840(10)	81.504(4)
γ (deg)	90	75.748(4)
V (Å^3)	1082.06(9)	684.1(3)
Z	2	1
Temperature (K)	100(2)	100(2)
ρcalc (Mg/m^3)	1.266	1.206
μ (mm^{-1})	0.074	0.070
θ range for data collection (deg)	1.287 to 26.136	1.575 to 26.124
Radiation	Mo Kα	Mo Kα
[I>2σ(I)]	$R_1 = 0.0350$ $wR_2 = 0.0915$	$R_1 = 0.0891$ $wR_2 = 0.1620$
R indices (all data)	$R_1 = 0.0401$ $wR_2 = 0.0959$	$R_1 = 0.1492$ $wR_2 = 0.1822$
GoF	1.051	1.084
CCDC	2277359	2277357

For **BPA**, **anthrarufin**, **anthraquinone**, and **DCAQ**, unit cell parameters obtained from our diffraction data matched those reported in the literature. As a result, full solutions of these crystals were not sought.

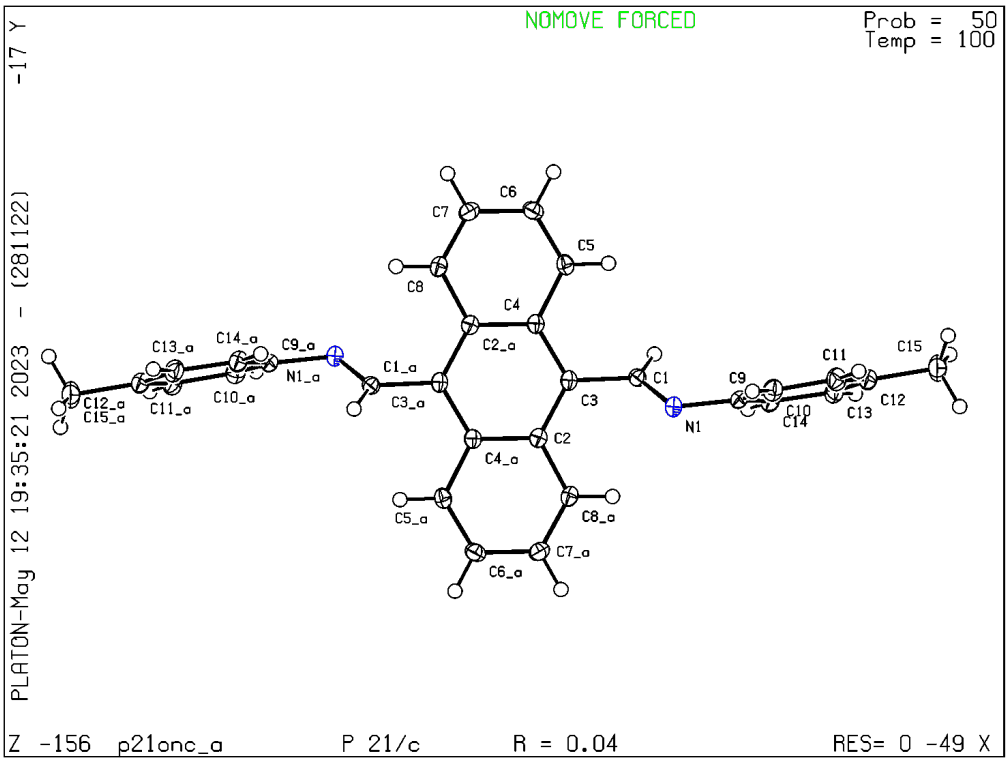

Figure S1: ORTEP diagram for the single crystal structure of **A-Me**.

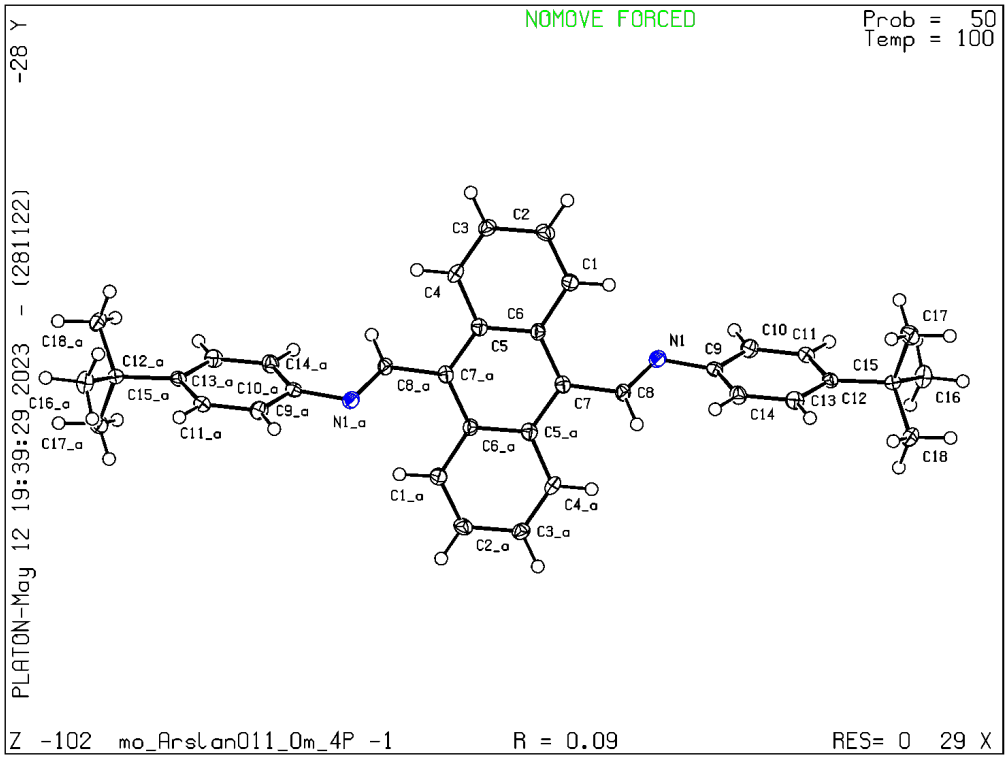

Figure S2: ORTEP diagram for the single crystal structure of **A-*t*Bu**.

For the single crystal growth of host-guest complexes of **A-Me** and **A-*t*Bu**, a saturated solution of the guest in **ExBox·4X** (5.00 mM, MeCN) was prepared. The excess solid was removed by filtration through a 0.22 μm hydrophilic PTFE filter, and the solution was transferred to a 1 mL glass culture tube (ID = 5mm). Single crystals were grown through slow diffusion of *i*Pr$_2$O in a 20 mL scintillation vial on benchtop at room temperature over 1-3 days. PF_6^- salt of **ExBox^{4+}** was used for the inclusion complex of **A-*t*Bu**. $TFSI^-$ salt of **ExBox^{4+}** was used for the inclusion complex of **A-Me**. For the single crystal growth of host-guest complex of **A-H**, a crystallization was performed directly from a one pot *in situ* synthesis, where **ExBox·4TFSI** (10.0 mM, MeCN) was combined with **ADC** (1 equiv.), aniline (5 equiv.) and $Sc(Otf)_3$ (1.0 equiv.) in the presence of 3Å molecular sieves, followed by slow diffusion of *i*Pr$_2$O over 1-3 days.

Table S2. Single crystal structure data of inclusion (host-guest) complexes.

	A-H⊂ExBox·4TfO 2C$_6$H$_5$NH$_2$	**A-Me⊂ExBox·4TFSI 2CH$_3$CN**	**A-*t*Bu⊂ExBox·4PF$_6$ 10CH$_3$CN**
Formula	$C_{92}H_{74}F_{12}N_8O_{12}S_4$	$C_{90}H_{70}F_{24}N_{12}O_{16}S_8$	$C_{104}H_{106}F_{24}N_{16}P_4$
Formula weight	1839.83	2288.06	2159.92
Space group	$P2_1/n$	$P\bar{1}$	$P\bar{1}$
Crystal system	Monoclinic	Triclinic	Triclinic
a (Å)	11.6339(17)	11.6487(8)	14.4346(2)
b (Å)	20.236(3)	12.2187(9)	19.1010(3)
c (Å)	18.043(3)	17.8531(13)	21.5810(4)
α (deg)	90	74.7070(10)	68.0780(10)
β (deg)	102.544(3)	73.7410(10)	72.5220(10)
γ (deg)	90	84.2490(10)	89.7170(10)
V (Å^3)	4146.4(10)	2352.1(3)	5226.35(15)
Z	2	1	2
Temperature (K)	100(2)	100(2)	100(2)
ρcalc (Mg/m^3)	1.474	1.615	1.373
μ (mm^{-1})	0.212	0.311	1.518
θ range for data collection (deg)	1.533 to 26.089	1.226 to 26.082	2.331 to 71.862
Radiation	Mo Kα	Mo Kα	Cu Kα
[I>2σ(I)]	R_1 = 0.0376 wR_2 = 0.0927	R_1 = 0.0289 wR_2 = 0.0766	R_1 = 0.0961 wR_2 = 0.2613
R indices (all data)	R_1 = 0.0482 wR_2 = 0.0993	R_1 = 0.0330 wR_2 = 0.0793	R_1 = 0.1015 wR_2 = 0.2712
GoF	1.028	1.030	1.063
CCDC	2277358	2277355	2277356

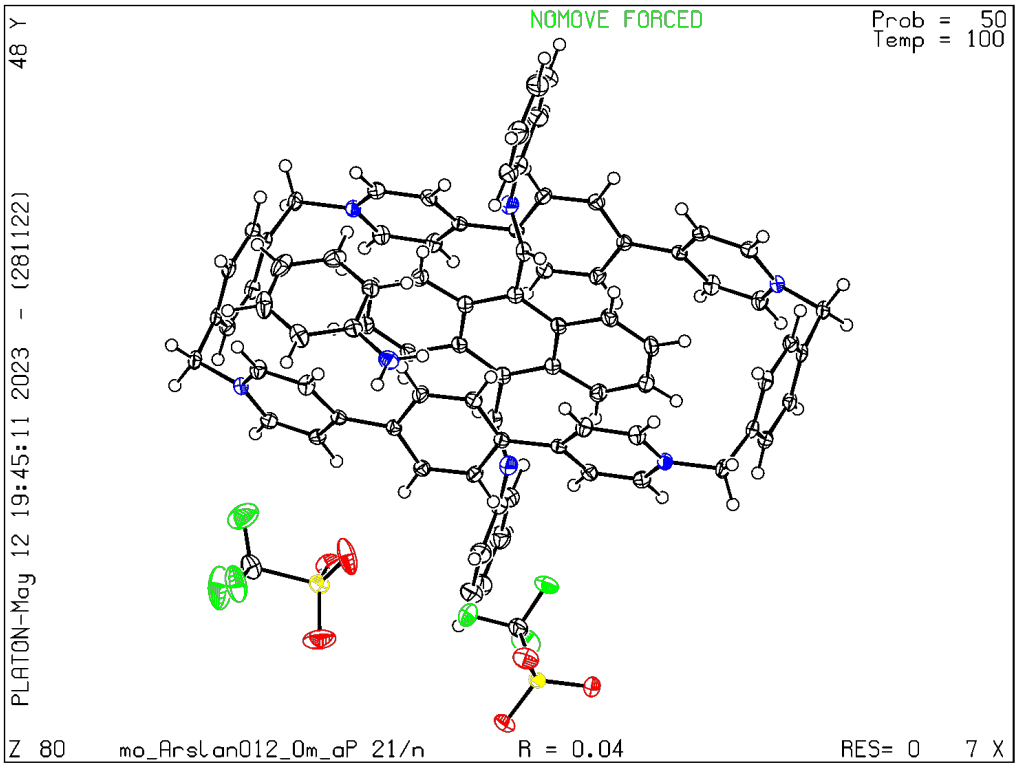

Figure S3: ORTEP diagram for the single crystal structure of **A-H⊂ExBox·4TfO**.

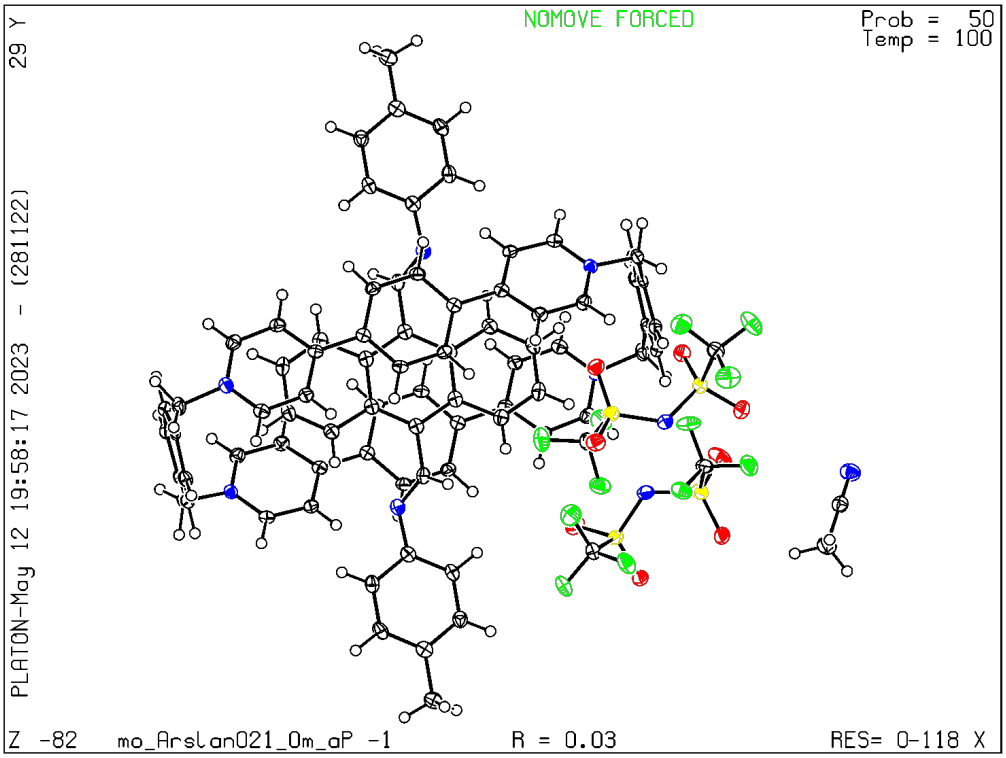

Figure S4: ORTEP diagram for the single crystal structure of **A-Me⊂ExBox·4TFSI**.

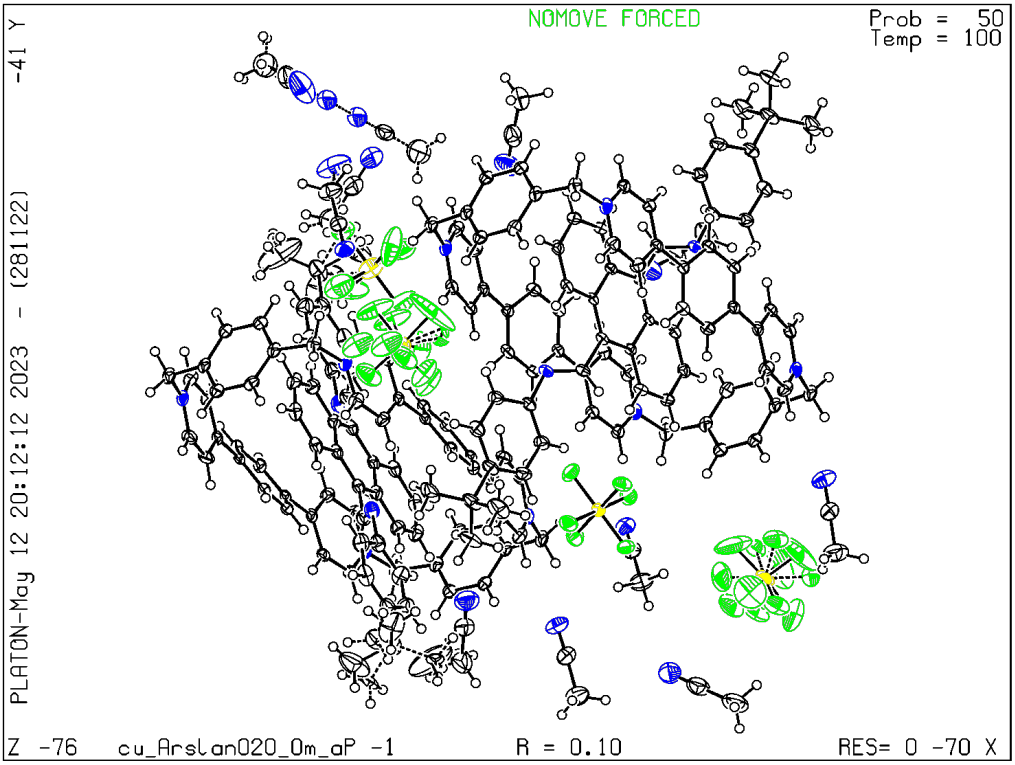

Figure S5: ORTEP diagram for the single crystal structure of **A-*t*Bu⊂ExBox·4PF$_6$**.

D. Solubility and Binding Measurements

For a more quantitative analysis of the displacement crystal growth process, solubilities of the guest molecules used in crystal growths, as well as their binding affinities to $ExBox^{4+}$ were studied using ^1H NMR spectroscopy. All measurements were done using a 90° pulse and a relaxation delay > $5\times T_1$ to ensure the integrations were suitable for qNMR.[8]

i) Solubility

To measure the solubility of each compound without $ExBox^{4+}$, a saturated solution in MeCN-d3 was prepared at 25 °C, and its concentration was determined against $(CH_3)_2SO_2$, an internal standard. A sample spectrum and calculation are shown below for A-Me.

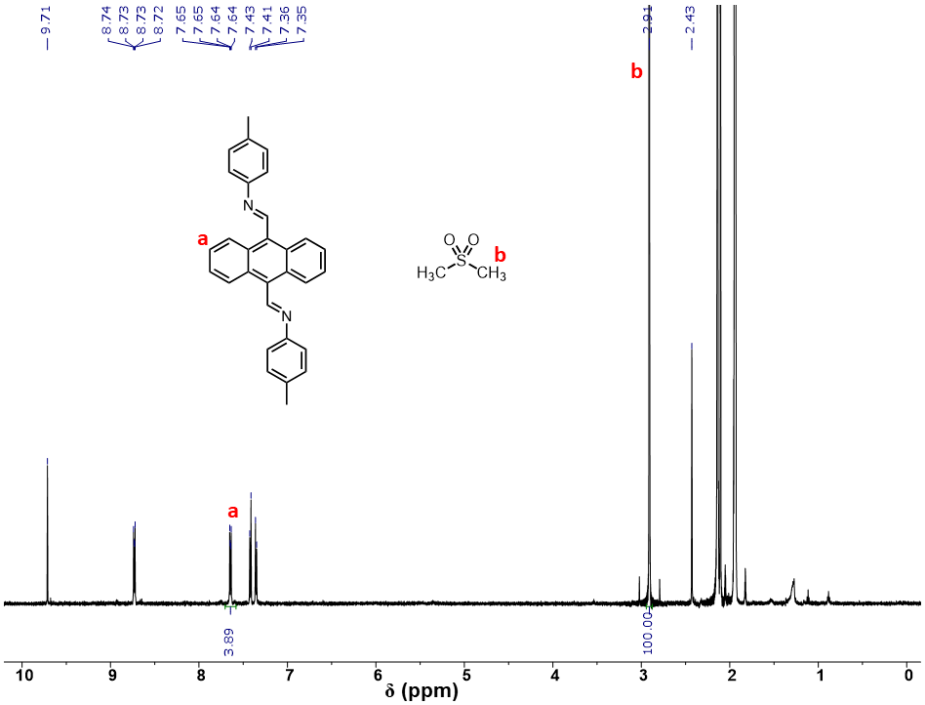

Figure S6. ^1H NMR of **A-Me** (600 MHz, MeCN-d3, 298 K). The internal standard is $(CH_3)_2SO_2$ with a concentration of 5.30 mM.

$$[A-Me]_{sat} = [DMSO_2] \times \frac{\int a\,/4}{\int b\,/4}$$

where,

$[A\text{-}Me]_{sat}$ = concentration of A-Me in MeCN-d3 in a saturated solution at 25 °C. This value is assumed to be equal to the solubility of A-Me in MeCN at this temperature.

$[DMSO_2]$ = 5.3 mM, concentration of the internal standard $(CH_3)_2SO_2$, dimethyl sulfone.

$\int a$ or $\int b$ = The integration values of peaks for the designated protons. Each integration value is normalized by dividing it by the number of protons that corresponds to that signal.

Entering the experimental values, the solubility of A-Me is found as:

$$[A-Me]_{sat} = [5.30\ mM] \times \frac{3.89/4}{100/6} = \mathbf{0.31\ mM}$$

This measurement was done at least three times for each compound, the averages and standard deviations were calculated and reported in Tables 1 and S3.

ii) Binding constants

A host:guest ratio of 1:1 was assumed for each of the host-guest complexes, which is well established in the literature for the complexes of $ExBox^{4+}$ in solution.[7] A binding constant, K_a , was determined for each guest compound according to the following equilibrium:

$$ExBox^{4+} + G \rightleftharpoons G\subset ExBox^{4+} \qquad K_a = \frac{[G\subset ExBox^{4+}]}{[G]\,[ExBox^{4+}]}$$

To measure the binding constant of each compound with $ExBox^{4+}$, a saturated solution of the guest was prepared in a 5.0mM ExBox·4TFSI solution in MeCN-d3 at 25 °C, and its concentration was determined against $ExBox^{4+}$. A sample spectrum and calculation are shown below for A-Me.

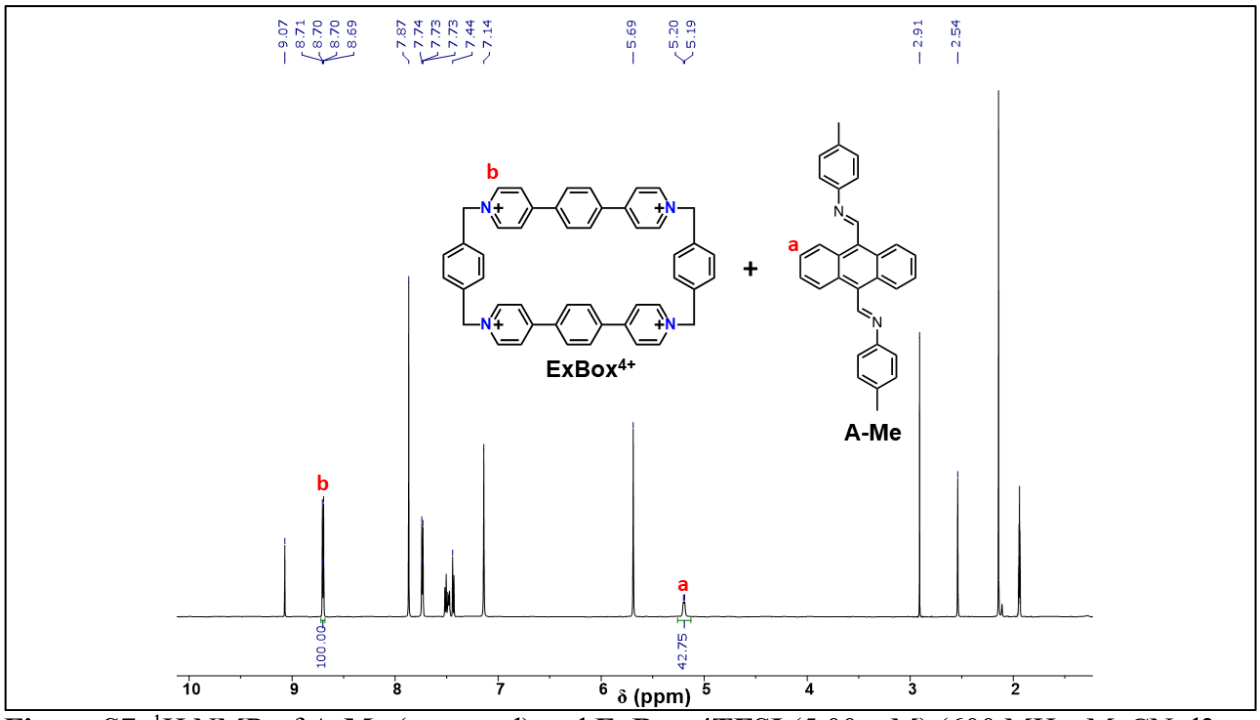

Figure S7. ^{1}H NMR of **A-Me** (saturated) and **ExBox·4TFSI** (5.00 mM) (600 MHz, MeCN-d3, 298 K).

$$[A-Me]_{tot} = [ExBox^{4+}]_{tot} \times \frac{\int a\,/4}{\int b\,/8}$$

where,

$[A\text{-}Me]_{tot}$ = total concentration of A-Me in a 5.00 mM ExBox·4TFSI solution in MeCN-d3 at 25 °C. This is equal to the initial concentration of A-Me before the equilibrium is reached.

$[ExBox^{4+}]_{tot}$ = 5.00 mM, total concentration of $ExBox^{4+}$. This is equal to the initial concentration of $ExBox^{4+}$ before the equilibrium is reached.

∫a or ∫b = The integration values of peaks for the designated protons. Each integration value is normalized by dividing it by the number of protons that corresponds to that signal. Integration values correspond to the total concentration of each discrete compound, as there is only one set of peaks for both the host and the guest because of the fast equilibrium, i.e. there is no separate set of peaks for the host-guest complex.

Entering the experimental values, the total concentration of A-Me is found as:

$$[A-Me]_{tot} = [5.00\ mM] \times \frac{42.75/4}{100/8} = \mathbf{4.28\ mM}$$

This measurement was done at least three times for each compound, the averages and standard deviations were calculated and reported in Tables 1 and S3.

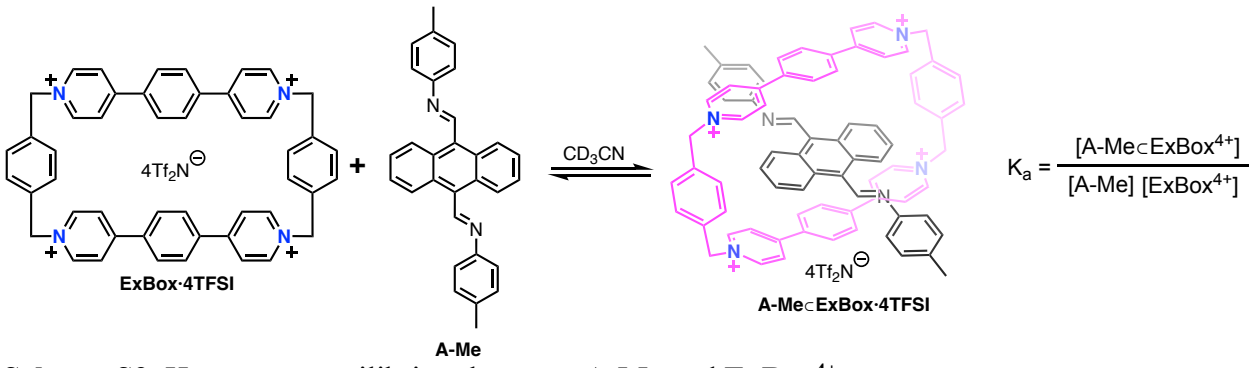

Scheme S2. Host-guest equilibrium between **A-Me** and **ExBox^{4+}**.

Under these equilibrium conditions, where there is an excess amount of A-Me solid present at the bottom of the NMR tube, it is assumed that the equilibrium concentration of A-Me is equal to the concentration of A-Me in its saturated solution without ExBox^{4+}:

$[\text{A-Me}]_{eq} = [\text{A-Me}]_{sat} = 0.37 \pm 0.04$ mM

As a result,

$[\text{A-Me}\subset\text{ExBox}^{4+}]_{eq} = [\text{A-Me}]_{tot} - [\text{A-Me}]_{eq} = 3.85 \pm 0.12$ mM

$[\text{ExBox}^{4+}]_{eq} = [\text{ExBox}^{4+}]_{tot} - [\text{A-Me}\subset\text{ExBox}^{4+}]_{eq} = 1.15 \pm 0.12$ mM

and $\boldsymbol{K_a} = \frac{[\text{A-Me}\subset\text{ExBox}^{4+}]_{eq}}{[\text{A-Me}]_{eq} \times [\text{ExBox}^{4+}]_{eq}} = (9.2 \pm 1.8) \times 10^3\ \boldsymbol{M^{-1}}$

iii) Binding constant (K_a) of A-Me with ExBox·4TFSI via ^{1}H NMR titration

In a typical titration, a saturated solution of A-Me in MeCN-d3 (0.5 mL) was filtered through a 0.22 µm hydrophilic PTFE filter and the concentration of A-Me was measured using an internal standard (dimethyl sulfone). This solution was titrated using a 5.00 mM solution of ExBox·4TFSI in MeCN-d3. The choice of titrating the guest with the host was based on the very low solubility of A-Me (0.37 ± 0.04 mM) under these conditions. This allowed for large equivalents (up to 5) of the host relative to the guest and obtain near-saturation conditions. The chemical shifts of the two peaks highlighted by a blue square and a green circle (Figure S8a) were tracked and plotted against the $[Host]_0/[Guest]_0$ ratio using BindFit v0.5 to obtain binding isotherms. A host:guest ratio of 1:1 was assumed, in accordance with our crystal structures and previously reported host-guest complexes of $ExBox^{4+}$. This process was repeated three times, giving an average binding constant, $\boldsymbol{K_a = 10.2 \pm 1.0 \times 10^3\ M^{-1}}$. This value is in good agreement with the value obtained using saturation concentrations, $\boldsymbol{K_a = 9.1 \pm 1.8 \times 10^3\ M^{-1}}$.

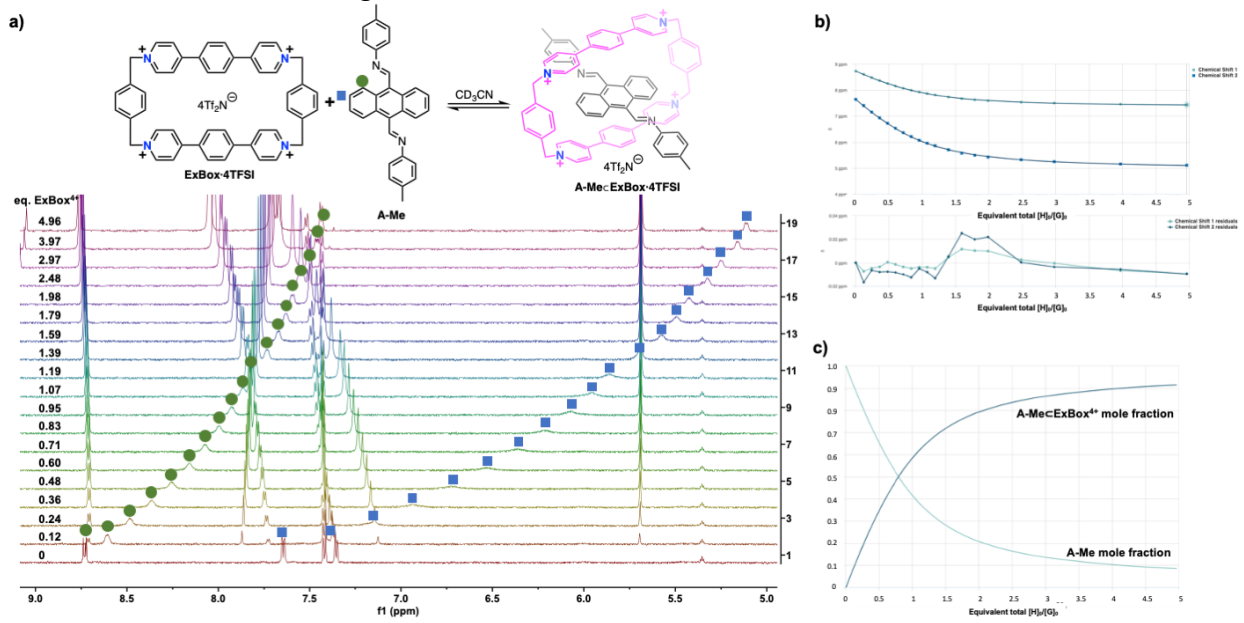

Figure S8. Binding titration of A-Me (0.39 mM) with ExBox·4TFSI (5.00 mM) via ^{1}H NMR spectroscopy (600 MHz, MeCN-d3, 298 K). **a)** ^{1}H NMR spectra of the mixture with increasing equivalents of ExBox·4TFSI, showing shifts in anthracene core peaks, **b)** Binding fits along with residuals, and **c)** Distribution of free and bound A-Me as a function of $[ExBox·4TFSI]_0/[A\text{-}Me]_0$ ratio.

iv) Binding constant (K_a) of A-H with ExBox·4TFSI via UV-vis absorption titration

In a typical titration, a 0.05 mM solution of A-H in MeCN was titrated with a 5.00 mM solution of ExBox·4TFSI in MeCN. Absorption values at 416 nm were plotted against the $[Host]_0/[Guest]_0$ ratio using BindFit v0.5 to obtain binding isotherms (Figure S9). A host:guest ratio of 1:1 was assumed. This process was repeated three times, giving an average binding constant, $K_a = 6.6 \pm 0.5 \times 10^3\ M^{-1}$.

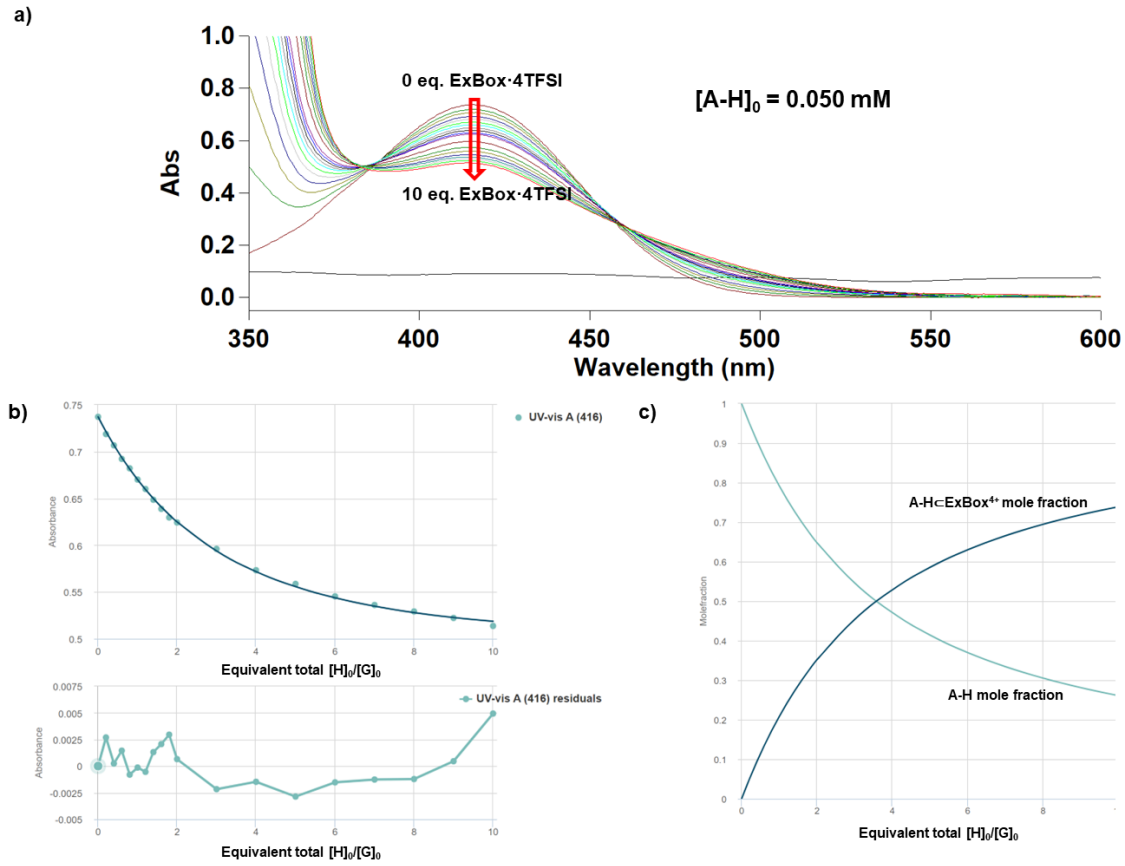

Figure S9. Binding titration of A-H (0.050 mM) with ExBox·4TFSI (5.00 mM) via UV-vis absorption spectroscopy (MeCN, 298 K). **a)** UV-vis absorption spectra of the mixture with increasing equivalents of ExBox·4TFSI, showing a decrease in absorbance at 416 nm, **b)** Binding fits along with residuals, and **c)** Distribution of free and bound A-H as a function of $[ExBox·4TFSI]_0/[A\text{-}H]_0$ ratio.

v) Solubility ratio

Our new crystal growth methodology depends on the inherent solubility differential of the guest compound with or without the host. Even though binding constant somewhat captures this difference, we defined a new parameter we call solubility ratio, S_r, as described below to directly measure it.

$$S_r = \frac{Total\ concentration\ of\ the\ guest\ in\ the\ presence\ of\ ExBox^{4+}}{Saturated\ concentration\ of\ the\ guest\ absent\ host}$$

For A-Me,

$$\boldsymbol{S_r}(A-Me) = \frac{[\mathrm{A-Me}]_{tot}}{[\mathrm{A-Me}]_{sat}} = \frac{4.22\ \pm\ 0.11\ \mathrm{mM}}{0.37\ \pm\ 0.04\ \mathrm{mM}} = \mathbf{11.5\ \pm\ 1.3}$$

Although $[\text{A-Me}]_{sat}$ is constant in a given solvent at a given temperature, $[\text{A-Me}]_{tot}$ is a function of the initial $ExBox^{4+}$ concentration, $[ExBox^{4+}]_{tot}$. As a result, S_r is not an intrinsic property and its value will change with $[ExBox^{4+}]_{tot}$. In order to compare the solubility ratios of different guests and better understand the guest-displacement crystal growth, it is necessary to use the same $[ExBox^{4+}]_{tot}$ concentration. This is why $[ExBox^{4+}]_{tot}$ = 5.00 mM was used for all equilibrium constant measurements.

Solubility, binding constant, and solubility ratio data for all the studied guests are summarized in Table S3.

Table S3. Solubility (c_{sat}), $c_{tot,}$ total concentration in the presence of 5.00 mM ExBox·4TFSI, solubility ratio (S_r), and binding constant (K_a) values for guests in MeCN-d3, along with the unit cell parameters of their crystals grown by controlled guest release.

Guest	c_{sat} ($\times 10^{-3}$ M)	c_{tot} ($\times 10^{-3}$ M)	S_r	K_a ($\times 10^3$ M^{-1})	Crystal information
A-*t*Bu	0.13 ± 0.03	3.32 ± 0.24	26.0 ± 5.6	13.8 ± 4.2	Yellow prisms, Triclinic $P\bar{1}$, a = 6.10 Å, b = 8.94 Å, c = 13.21 Å α = 79.84°, β = 81.50°, γ = 75.74°, V = 684 Å^3
BPA	0.15 ± 0.03	2.25 ± 0.38	15.0 ± 4.0	4.8 ± 1.9	Pale yellow needles, Orthorhombic *Pbcn*, a = 7.08 Å, b = 11.50 Å, c = 24.31 Å, V = 1978 Å^3 [9]
A-H	0.32 ± 0.13	4.05 ± 0.44	12.6 ± 5.1	6.6 ± 0.5[a]	[b]
A-Me	0.37 ± 0.04	4.22 ± 0.11	11.5 ± 1.3	9.2 ± 1.8[c]	Yellow plates, Monoclinic $P2_1/c$, a = 16.23 Å, b = 5.70 Å, c = 11.97 Å β = 102.98°, Volume = 1082 Å^3
Anthrarufin	0.52 ± 0.03	2.97 ± 0.22	5.7 ± 0.5	1.9 ± 0.4	Yellow-orange cubes, Monoclinic $P2_1/c$, a = 6.07 Å, b = 5.28 Å, c = 15.69 Å, β = 94.09° [10]
Alizarin	2.70 ± 0.07	5.60 ± 0.08	2.1 ± 0.1	0.5 ± 0.1	[d]
AQ	3.12 ± 0.23	6.26 ± 0.29	2.0 ± 0.2	0.5 ± 0.2	Colorless needles, Monoclinic $P2_1/c$, a = 15.76 Å, b = 3.97 Å, c = 15.78 Å, β = 102.69°, V = 963 Å^3 [11]
DCAQ	3.07 ± 0.14	5.93 ± 0.73	1.9 ± 0.3	0.4 ± 0.3	Yellow needles, Monoclinic $P2/c$, a = 3.86 Å, b = 10.40 Å, c = 13.69 Å, β = 93.39°, V = 549 Å^3 [12]
ADC	4.91 ± 0.86	8.60 ± 1.49	1.7 ± 0.4	2.3 ± 0.3[e]	[d]

[a] Binding constant was determined by UV-vis titration. [b] Crystals were small, thin, and highly twinned along the thin dimension. [c] Binding constant determined by ^{1}H-NMR titration is 10.2 ± 1.0 × 10^3 M^{-1}. [d] No crystal formation was observed. [e] Binding constant was determined by ^{1}H-NMR titration.

As can be seen from Table S3, S_r values are inversely correlated with the concentrations of the guests in their saturated solutions without any $ExBox^{4+}$ presence.

E. ^{1}H and ^{13}C NMR Spectroscopy

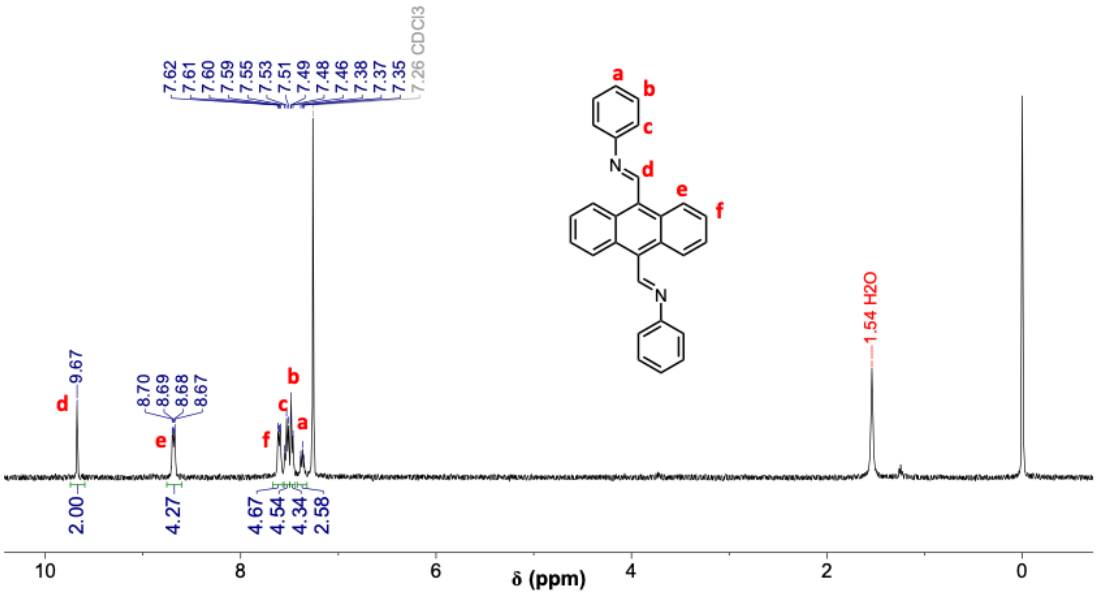

Figure S10. ^{1}H NMR of **A-H** (400 MHz, $CDCl_3$, 298 K).

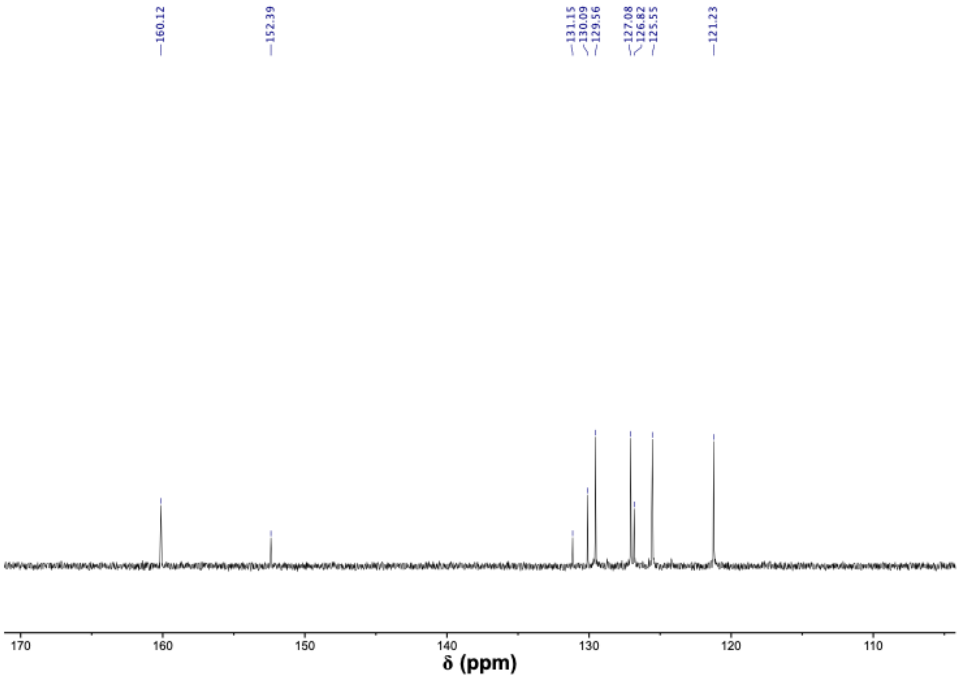

Figure S11. ^{13}C NMR of **A-H** (400 MHz, $CDCl_3$, 298 K).

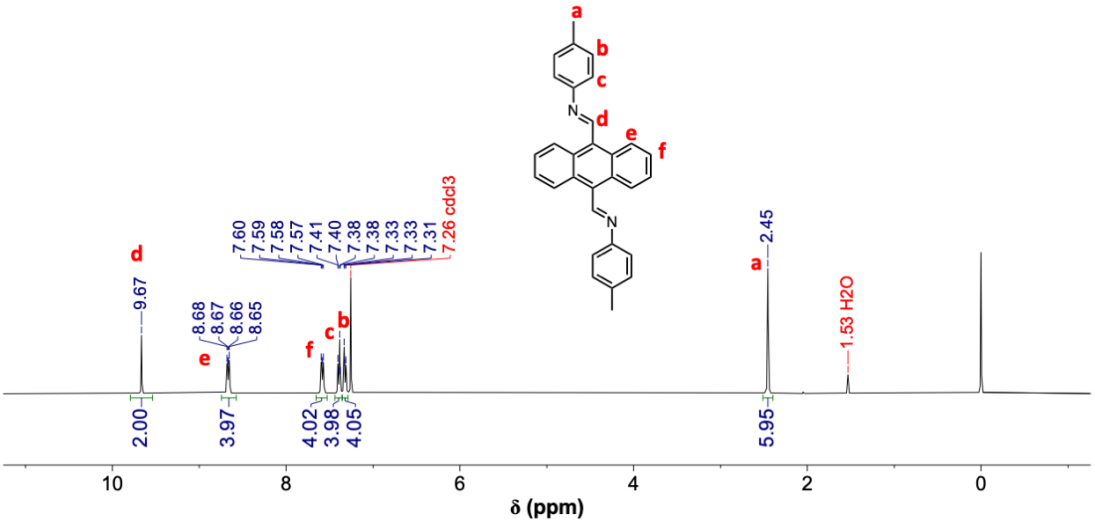

Figure S12. ^{1}H NMR of **A-Me** (400 MHz, $CDCl_3$, 298 K).

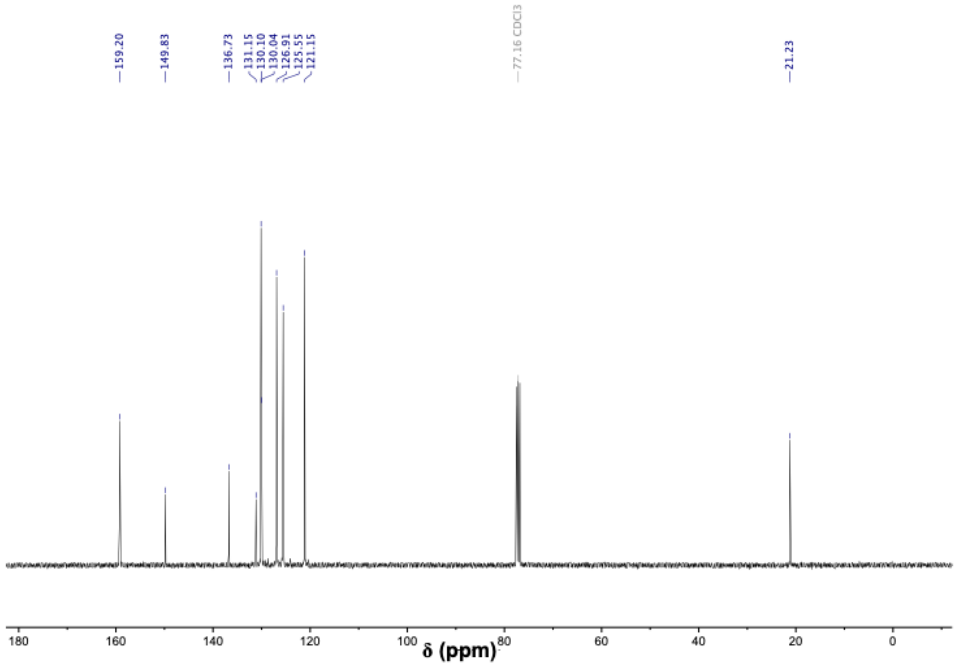

Figure S13. ^{13}C NMR of **A-Me** (400 MHz, $CDCl_3$, 298 K).

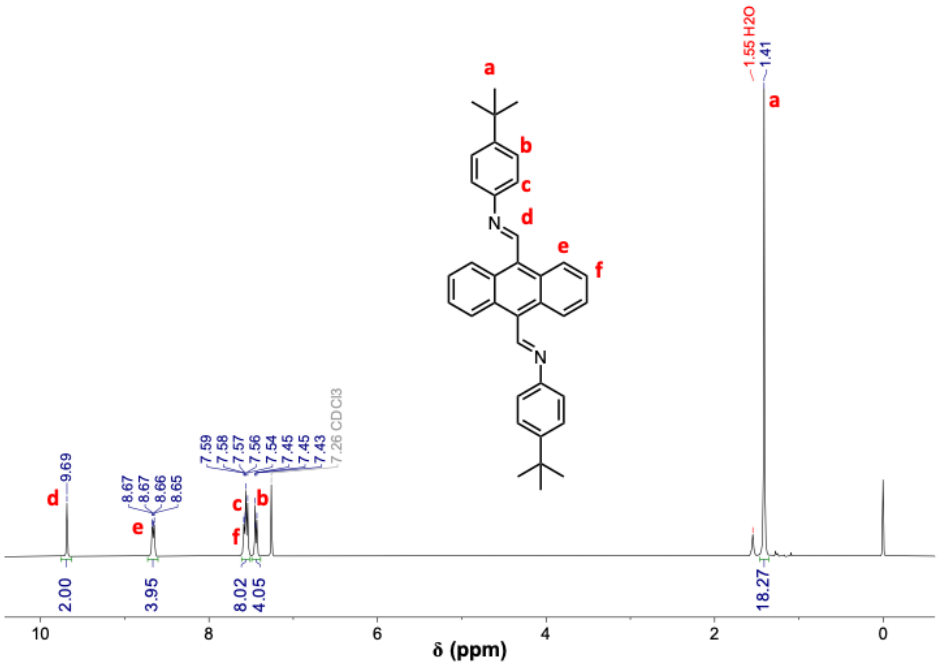

Figure S14. ^{1}H NMR of **A-*t*Bu** (400 MHz, $CDCl_3$, 298 K).

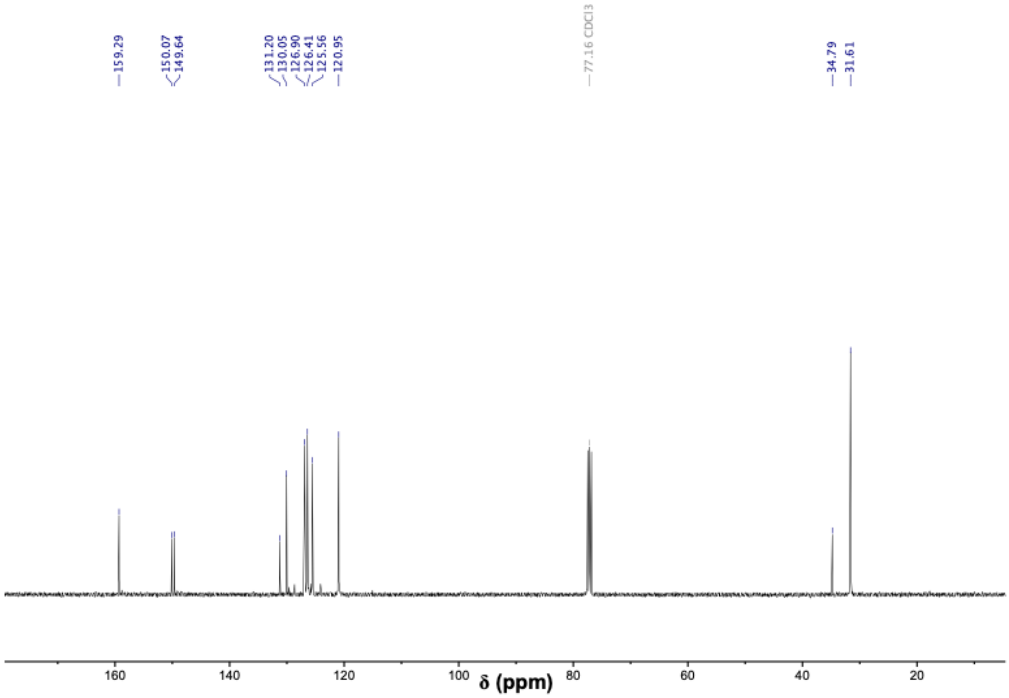

Figure S15. ^{13}C NMR of **A-*t*Bu** (400 MHz, $CDCl_3$, 298 K).

F. [1]H-NMR Spectra for Host-Guest Complexation

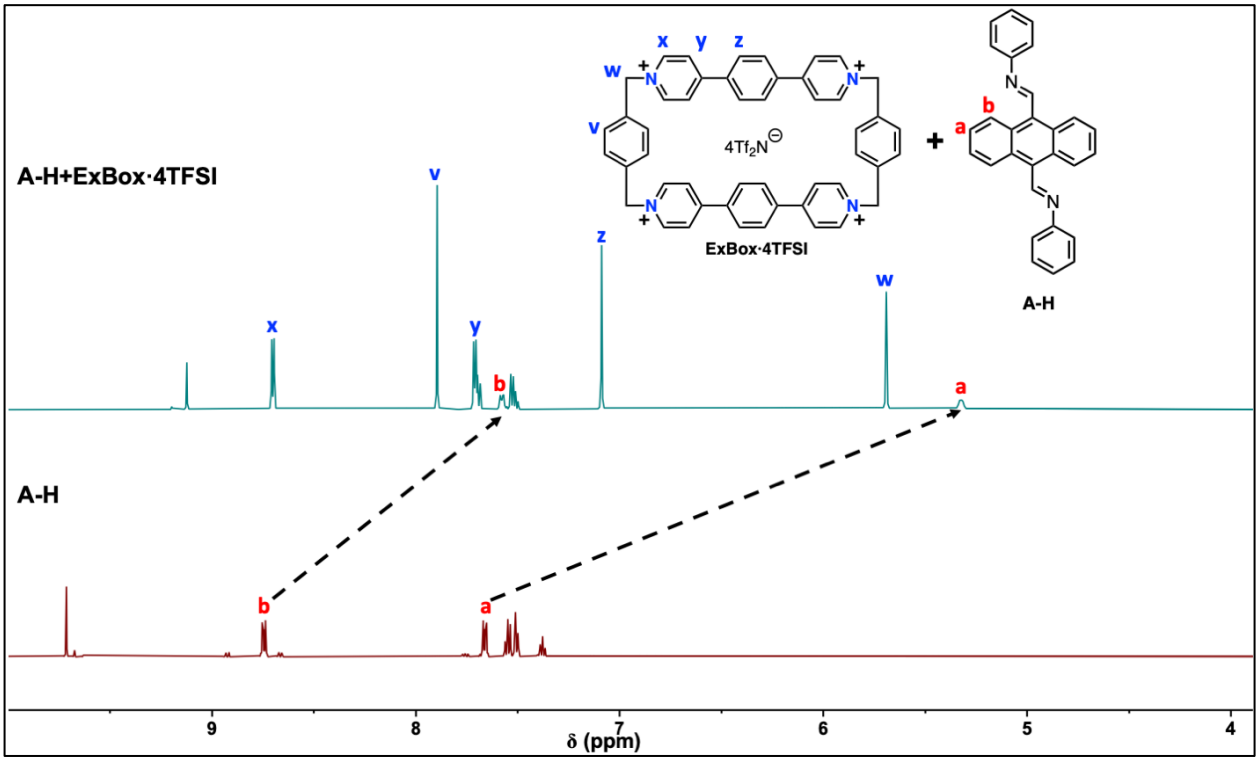

Figure S16. [1]H NMR of **A-H** and **A-H+ExBox·4TFSI** (600 MHz, MeCN-d3, 298 K).

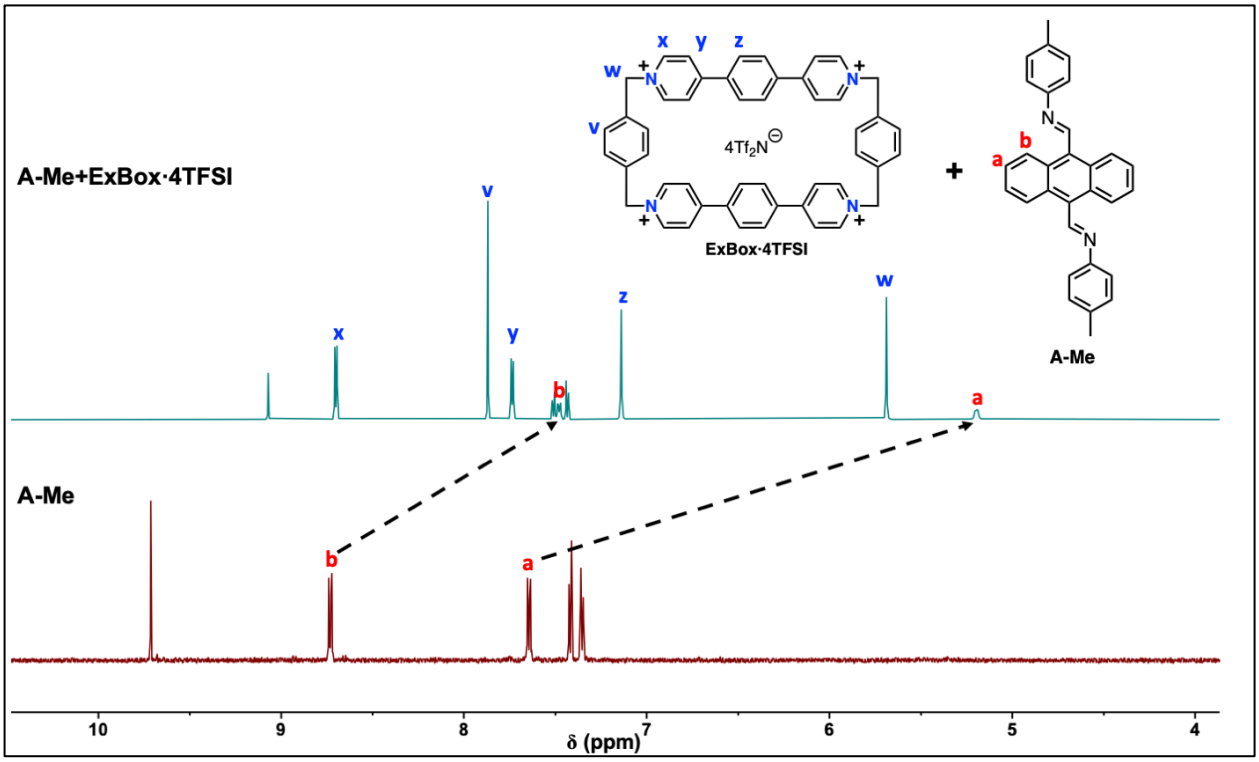

Figure S17. [1]H NMR of **A-Me** and **A-Me+ExBox·4TFSI** (600 MHz, MeCN-d3, 298 K).

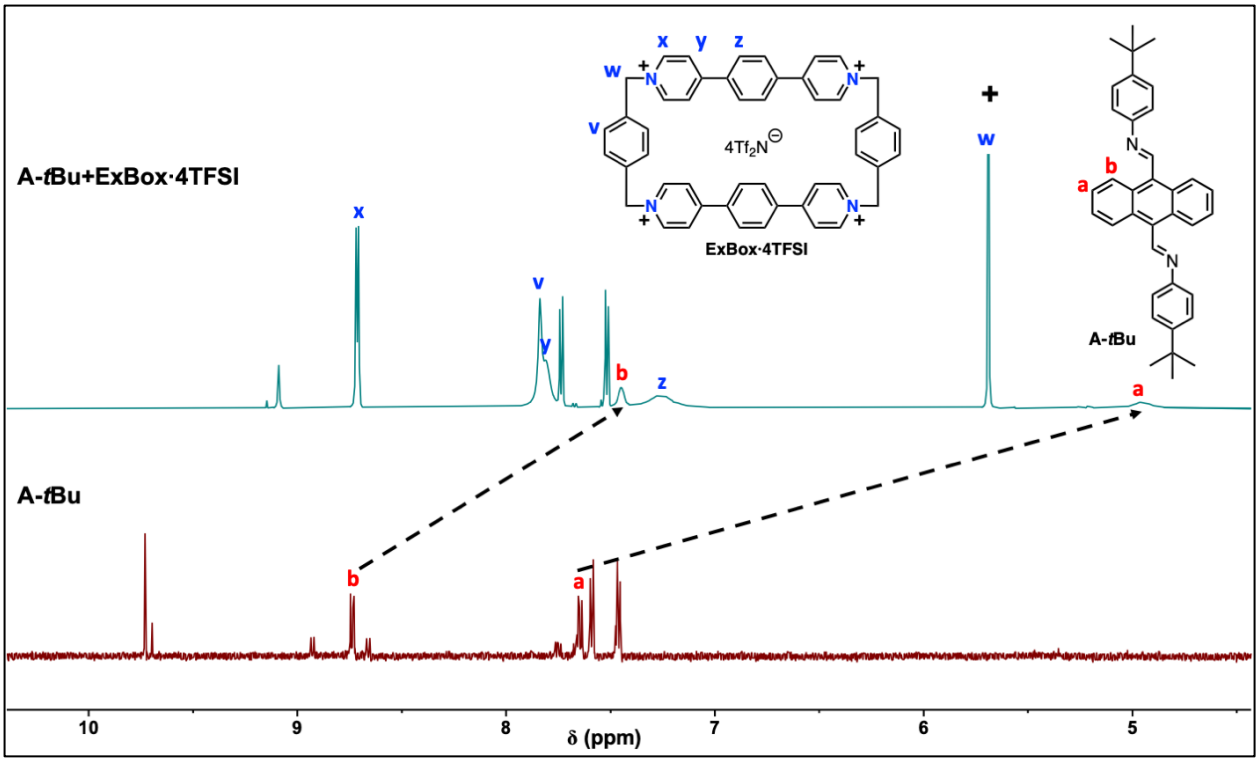

Figure S18. ^{1}H NMR of **A-*t*Bu** and **A- *t*Bu+ExBox·4TFSI** (600 MHz, MeCN-d3, 298 K).

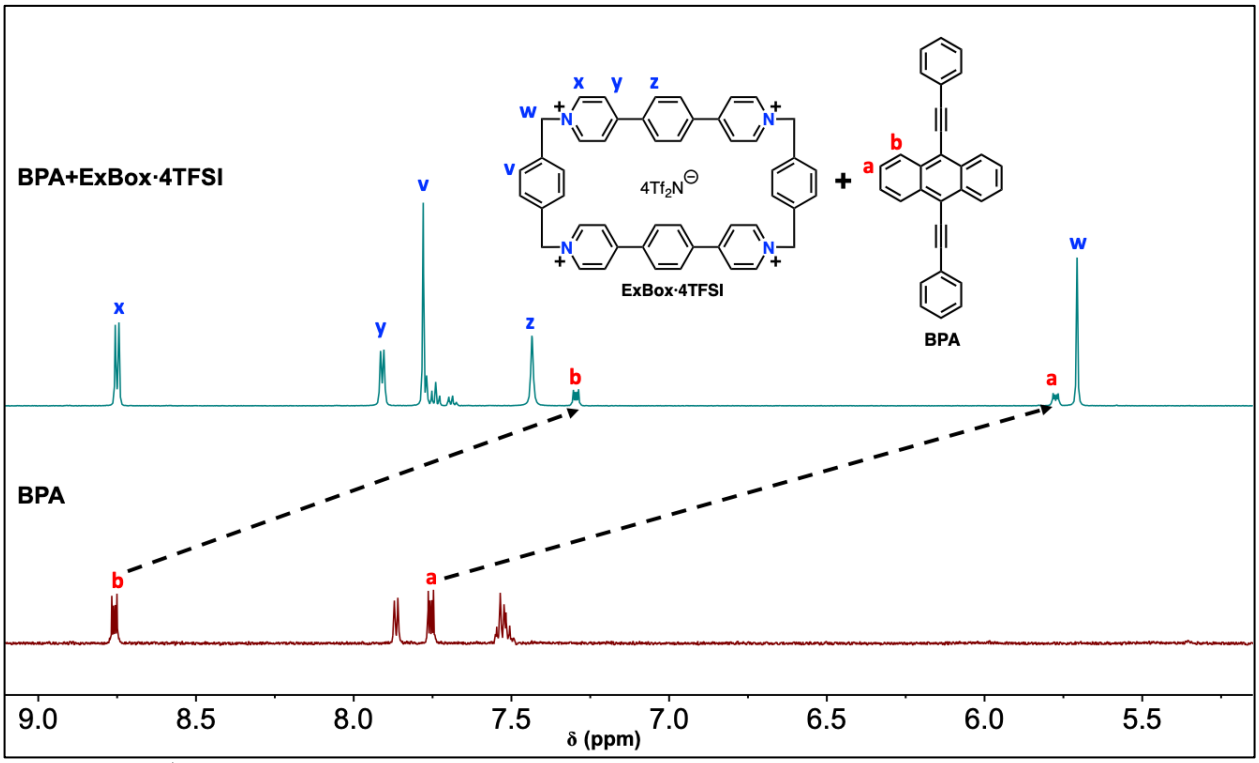

Figure S19. ^{1}H NMR of **BPA** and **BPA+ExBox·4TFSI** (600 MHz, MeCN-d3, 298 K).

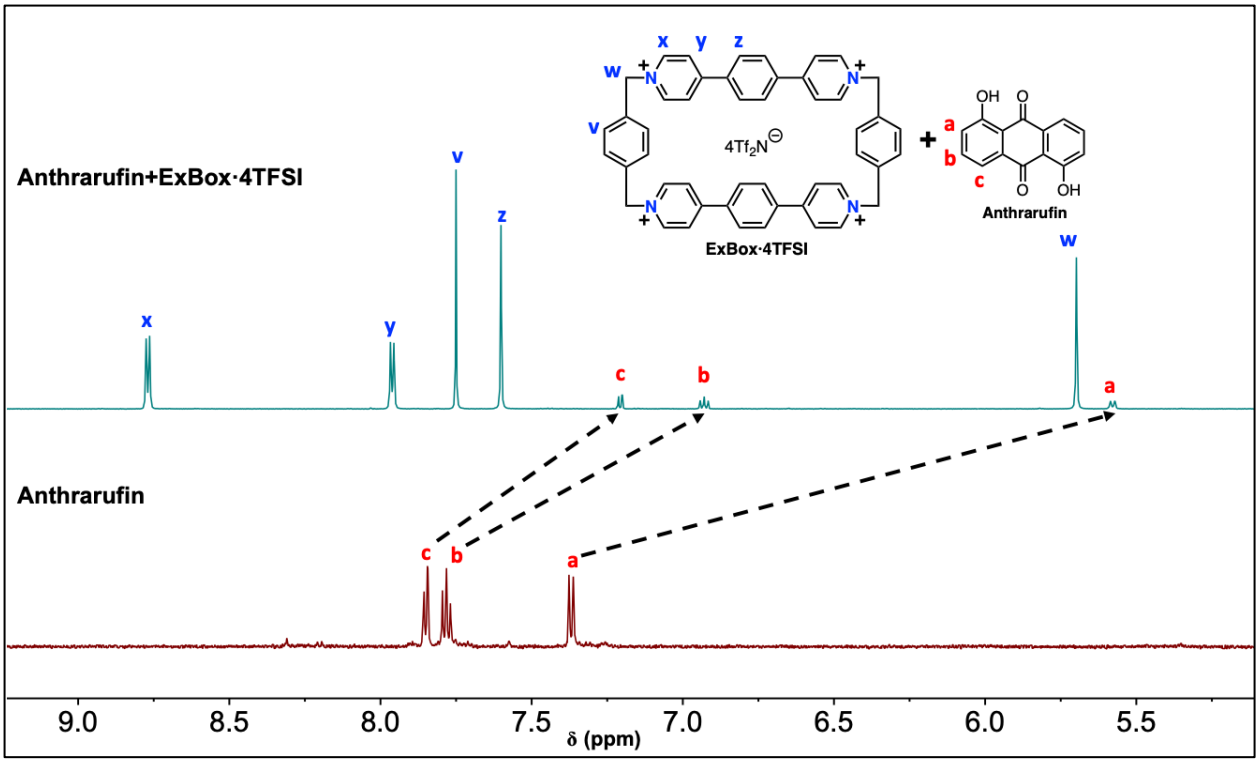

Figure S20. ^{1}H NMR of **anthrarufin** and **anthrarufin+ExBox·4TFSI** (600 MHz, MeCN-d3, 298 K).

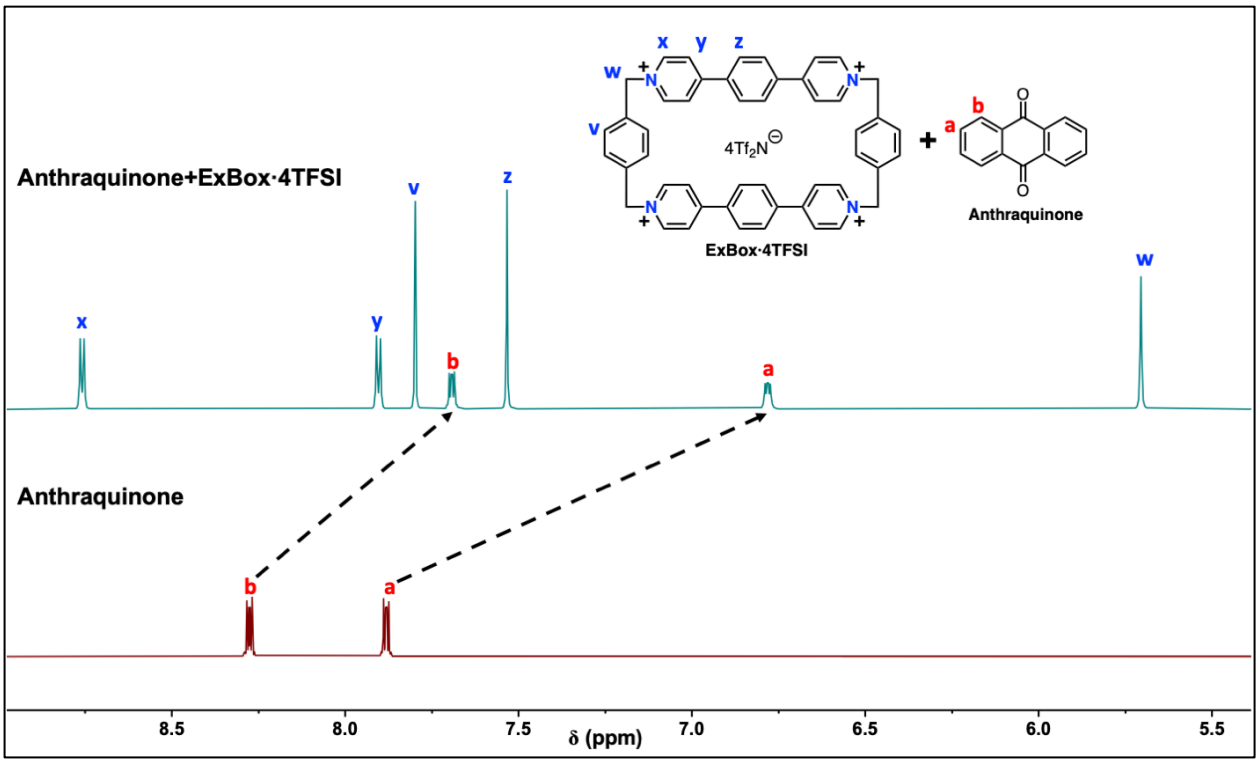

Figure S21. ^{1}H NMR of **anthraquinone** and **anthraquinone+ExBox·4TFSI** (600 MHz, MeCN-d3, 298 K).

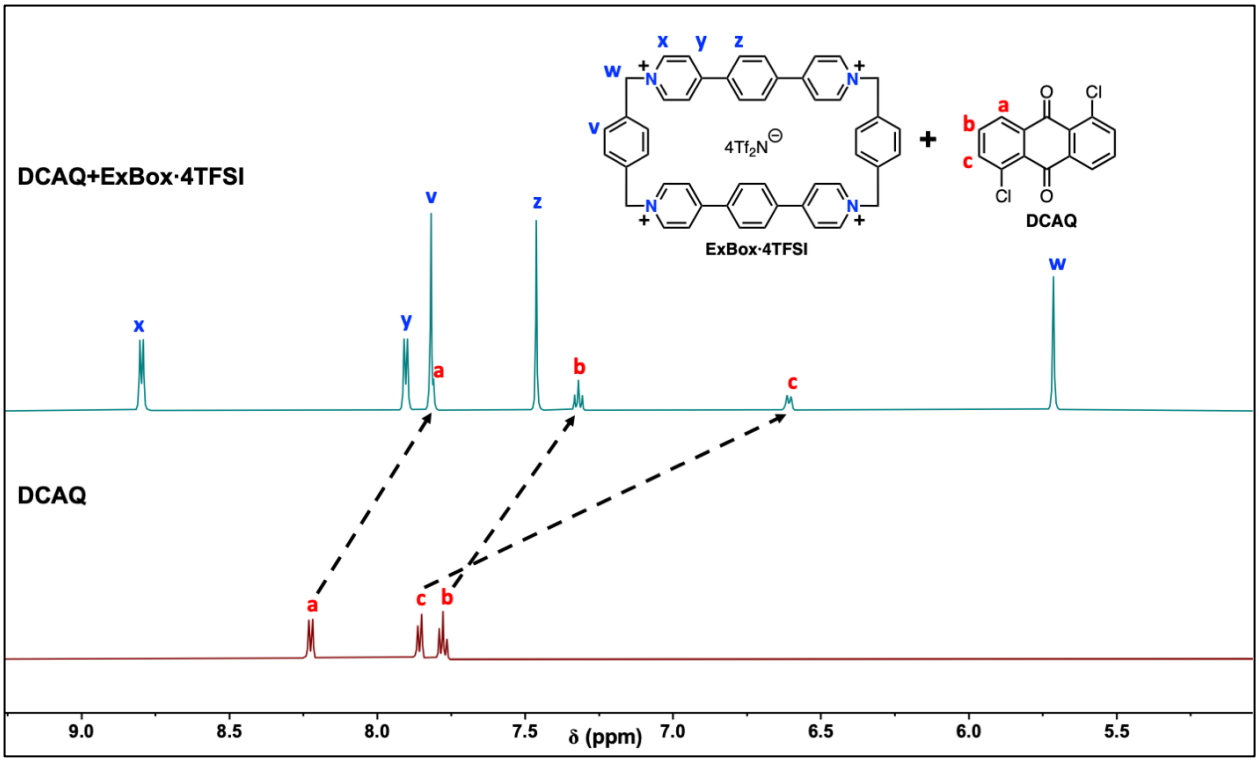

Figure S22. ^{1}H NMR of **DCAQ** and **DCAQ+ExBox·4TFSI** (600 MHz, MeCN-d3, 298 K).

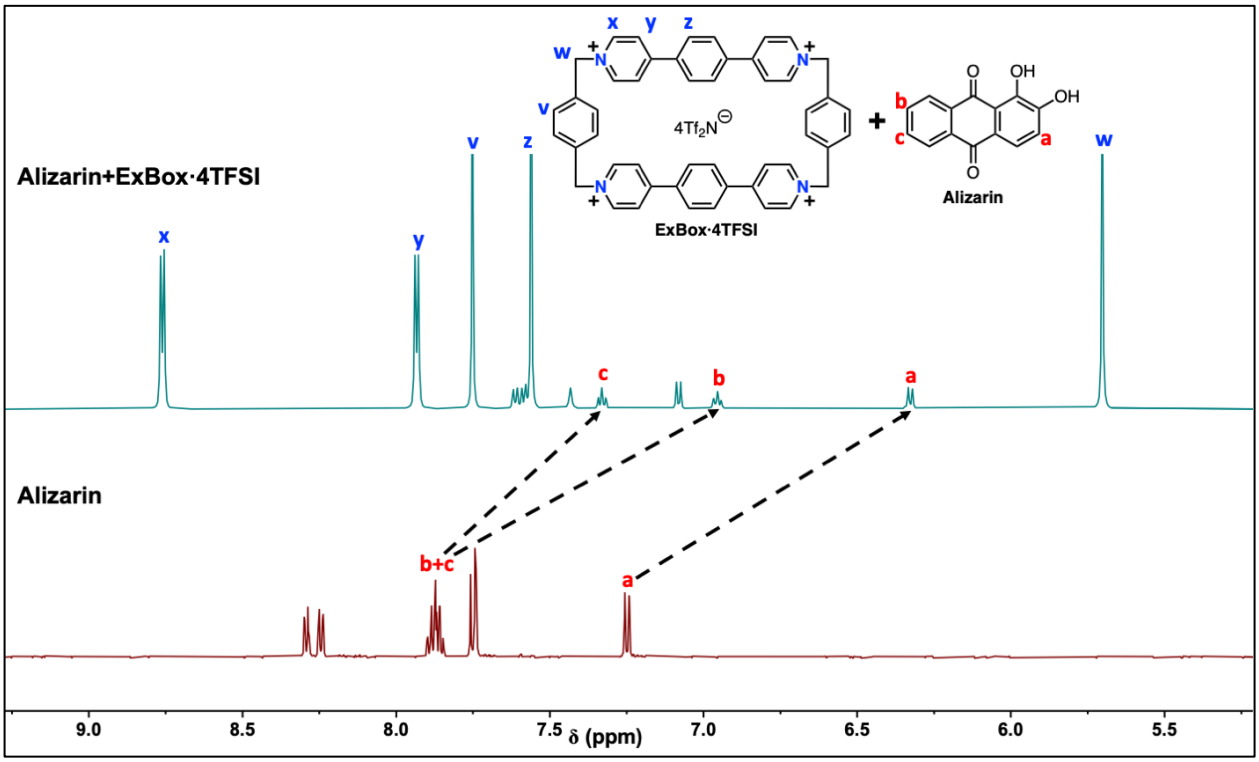

Figure S23. ^{1}H NMR of **alizarin** and **alizarin+ExBox·4TFSI** (600 MHz, MeCN-d3, 298 K).

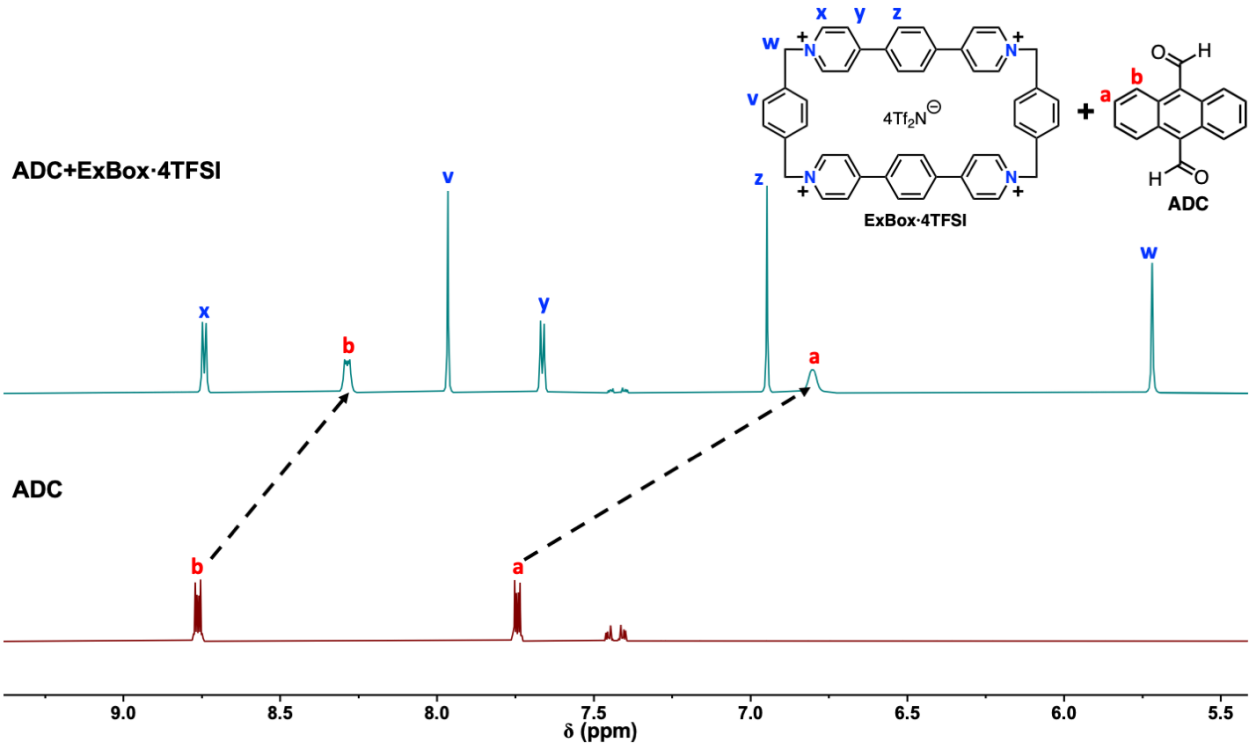

Figure S24. ^{1}H NMR of **ADC** and **ADC+ExBox·4TFSI** (600 MHz, MeCN-d3, 298 K).

G. Optical microscopy

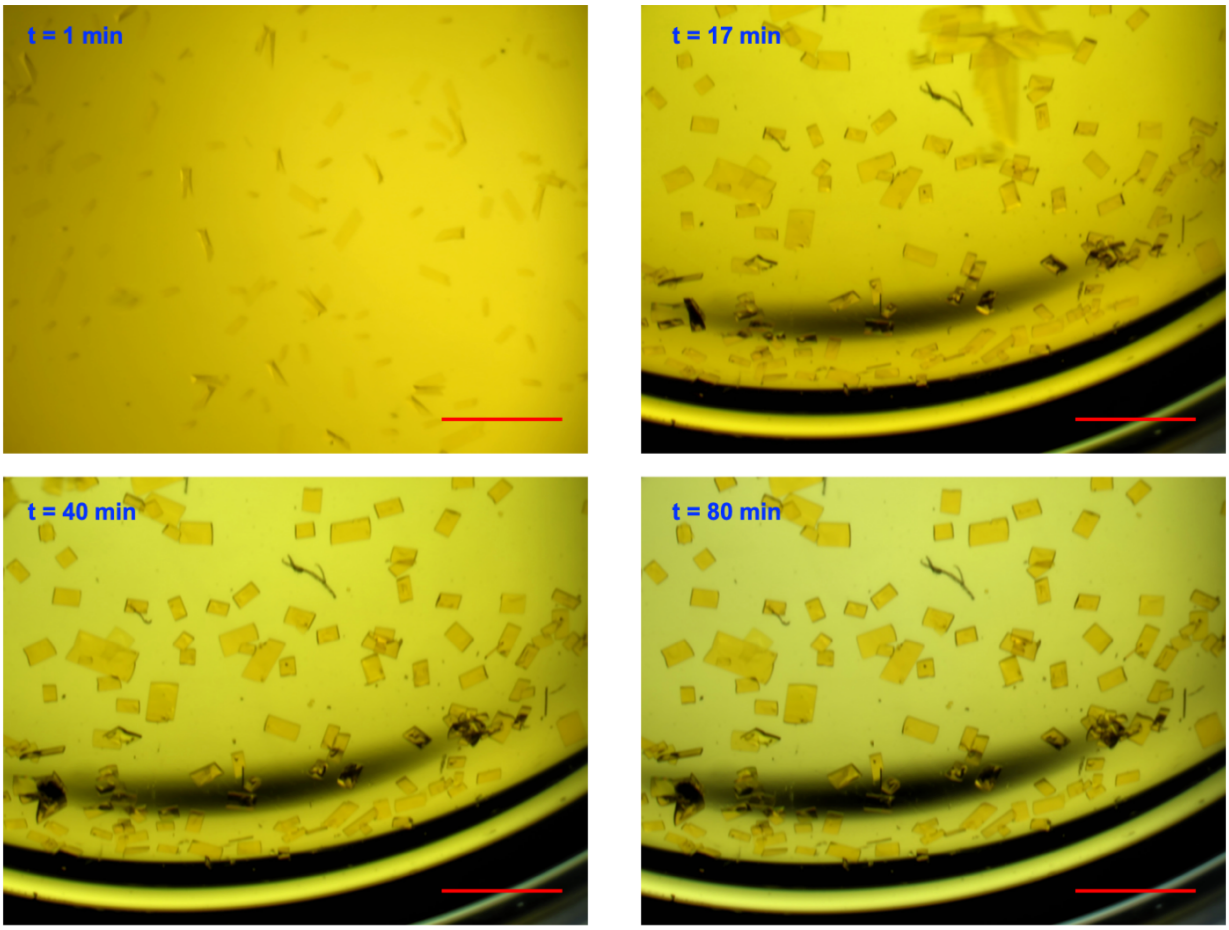

Figure S25. Optical microscopy images (scale bar, 1 mm) for the GuD growth of **A-*t*Bu** single crystals 1, 18, 40, and 80 minutes after the addition of 0.05 mL saturated pyrene solution (84 ± 10 mM in MeCN) to a 0.30 mL solution of **A-*t*Bu** (3.6 mM) and **ExBox·4TFSI** (5.0 mM) in MeCN in a 2-dram shell vial. Rapid crystal formation is observed initially, and the majority of the crystal growth is complete by 17 minutes. See included video of initial 17 minutes (shown at 20x speed).

H. References

(1) Barnes, J. C.; Juríček, M.; Vermeulen, N. A.; Dale, E. J.; Stoddart, J. F. Synthesis of ExnBox Cyclophanes. *J. Org. Chem.* **2013**, *78* (23), 11962–11969. https://doi.org/10.1021/jo401993n.

(2) Hibbert, D. B.; Thordarson, P. The Death of the Job Plot, Transparency, Open Science and Online Tools, Uncertainty Estimation Methods and Other Developments in Supramolecular Chemistry Data Analysis. *Chem. Commun.* **2016**, *52* (87), 12792–12805. https://doi.org/10.1039/C6CC03888C.

(3) *SAINT PLUS*: Bruker Analytical X-Ray Systems: Madison, WI, 2001.

(3) *SADABS*: Bruker Analytical X-Ray Systems: Madison, WI, 2001.

(5) Sheldrick, G. M. A Short History of SHELX. *Acta Crystallogr. A* **2008**, *64* (1), 112–122. https://doi.org/10.1107/S0108767307043930.

(6) Hübschle, C. B.; Sheldrick, G. M.; Dittrich, B. ShelXle: A Qt Graphical User Interface for SHELXL. *J. Appl. Crystallogr.* **2011**, *44* (6), 1281–1284. https://doi.org/10.1107/S0021889811043202.

(7) Barnes, J. C.; Juríček, M.; Strutt, N. L.; Frasconi, M.; Sampath, S.; Giesener, M. A.; McGrier, P. L.; Bruns, C. J.; Stern, C. L.; Sarjeant, A. A.; Stoddart, J. F. ExBox: A Polycyclic Aromatic Hydrocarbon Scavenger. *J. Am. Chem. Soc.* **2013**, *135* (1), 183–192. https://doi.org/10.1021/ja307360n.

(8) *Rapid Estimation of T1 for Quantitative NMR | The Journal of Organic Chemistry*. https://pubs.acs.org/doi/10.1021/acs.joc.1c01007 (accessed 2023-06-13).

(9) Karothu, D. P.; Dushaq, G.; Ahmed, E.; Catalano, L.; Rasras, M.; Naumov, P. Multifunctional Deformable Organic Semiconductor Single Crystals. *Angew. Chem. Int. Ed.* **2021**, *60* (50), 26151–26157. https://doi.org/10.1002/anie.202110676.

(10) Wei, G.-Q.; Yu, Y.; Zhuo, M.-P.; Wang, X.-D.; Liao, L.-S. Organic Single-Crystalline Whispering-Gallery Mode Microlasers with Efficient Optical Gain Activated via Excited State Intramolecular Proton Transfer Luminogens. *J. Mater. Chem. C* **2020**, *8* (34), 11916–11921. https://doi.org/10.1039/D0TC02881A.

(11) Chen, Y.-J.; Yang, S.-C.; Tsai, C.-C.; Chang, K.-C.; Chuang, W.-H.; Chu, W.-L.; Kovalev, V.; Chung, W.-S. Anthryl-1,2,4-Oxadiazole-Substituted Calix[4]Arenes as Highly Selective Fluorescent Chemodosimeters for Fe3+. *Chem. – Asian J.* **2015**, *10* (4), 1025–1034. https://doi.org/10.1002/asia.201403265.

(12) Wang, P.-W. A Solid-State Transformation in 1,5-Dichloroanthraquinone. *J. Appl. Crystallogr.* **1979**, *12* (2), 239–239. https://doi.org/10.1107/S002188987901222X.